cosmetics

MDPI

Article

Nanocellulose-Stabilized Pickering Emulsions for Cosmetic Applications

Ana Júlia Vaz de Melo Soares [1,2], Dislyane Trajano da Silva [2,3], Maryana Rogéria dos Santos [2,4], Gleice Paula de Araújo [2,4], Andréa Fernanda de Santana Costa [2,5], Attilio Converti [2,6], Italo José Batista Durval [2,3] and Leonie Asfora Sarubbo [2,3,*]

1 Center for Technology and Geosciences, Department of Chemical Engineering, Federal University of Pernambuco (UFPE), Av. dos Economistas, Cidade Universitária, Recife 50670-901, PE, Brazil; julia.vaz@ufpe.br
2 Advanced Institute of Technology and Innovation (IATI), Rua Potyra, 31, Prado, Recife 50751-310, PE, Brazil; dislyane.00000854534@unicap.br (D.T.d.S.); santosrmaryana@gmail.com (M.R.d.S.); gleice.araujo@iati.org.br (G.P.d.A.); andrea.santana@ufpe.br (A.F.d.S.C.); converti@unige.it (A.C.); italo.durval@iati.org.br (I.J.B.D.)
3 School of Technology and Communication, Catholic University of Pernambuco (UNICAP), Rua do Príncipe, 526, Boa Vista, Recife 50050-900, PE, Brazil
4 Northeast Biotechnology Network (RENORBIO), Federal Rural University of Pernambuco (UFRPE), Rua Dom Manuel de Medeiros, s/n, Dois Irmãos, Recife 52171-900, PE, Brazil
5 Center for Communication and Design, Academic Center of the Agreste Region, Federal University of Pernambuco (UFPE), BR 104, km 59, s/n, Nova Caruaru, Caruaru 55014-900, PE, Brazil
6 Department of Civil, Chemical and Environmental Engineering, University of Genoa (UNIGE), Pole of Chemical Engineering, Via Opera Pia, n. 15, 16145 Genoa, Italy
* Correspondence: leonie.sarubbo@unicap.br

Abstract

The development of innovative cosmetic ingredients has driven growing interest in emulsion systems that combine performance, stability, and sustainability. Pickering emulsions can form physically stable systems by adsorbing solid particles at the oil–water interface. In this study, bacterial cellulose nanofibers (CNFs) and nanocrystals (CNCs), obtained via acid hydrolysis, were evaluated as stabilizing agents in Pickering emulsions containing jojoba, castor, and grape seed oils for hair conditioning applications. Structural and physicochemical characterization revealed that CNCs exhibited higher crystallinity, a narrower size distribution, and a higher negative surface charge than CNFs, resulting in enhanced colloidal stability. Emulsion analyses showed that CNCs more effectively reduced interfacial tension and produced smaller, more homogeneous droplets. Stability assessments under pH variation, thermal stress, and storage demonstrated that CNC-stabilized emulsions, particularly with castor oil, maintained stability indices above 95% for up to 60 days, whereas CNF-based systems showed greater sensitivity to environmental conditions. The incorporation of CNCs into a prototype conditioning cream resulted in a creamy texture and improved physical stability without compromising formulation performance. Overall, these results highlight CNCs as robust and efficient stabilizing materials for Pickering emulsions, reinforcing the potential of bacterial nanocellulose in advanced cosmetic formulations.

Keywords: cellulose nanocrystals; cosmetic formulations; sustainable materials

Academic Editor: Luis Alfonso Trujillo-Cayado

Received: 26 December 2025
Revised: 20 January 2026
Accepted: 27 January 2026
Published: 30 January 2026

1. Introduction

The Brazilian cosmetics market is expanding rapidly, making Brazil the third-largest global market for beauty and personal care, according to data from the Brazilian Association of the Personal Hygiene, Perfumery, and Cosmetics Industry (ABIHPEC) [1]. Emulsions are multiphase colloidal systems typically formed by mixing two liquids: one with a dispersed phase and one with a continuous phase [2,3]. The use of emulsions is essential across various industrial sectors, including the pharmaceutical, food, cosmetic, and agricultural industries. In the food sector, emulsions are widely employed to extend shelf life while enhancing flavor and texture, as seen in creams, desserts, preserves, and other foods. In pharmaceuticals, emulsions can improve drug release and bioavailability. In cosmetics, they serve as a base for lotions, balms, soaps, and various other formulations [2,4].

Emulsions are thermodynamically stable systems prone to destabilization mechanisms like flocculation and Ostwald ripening [5]. Traditionally, their formation relies on surfactants; however, many of these agents have low biodegradability and cause harmful environmental effects [3], prompting the search for surfactant-free alternatives. In this regard, Pickering emulsions are notable as they are stabilized by solid particles adsorbed at the interface between mixed liquids, forming a rigid barrier that reduces interfacial tension and prevents processes like Ostwald ripening thanks to the irreversible adsorption of micro- or nanoparticles at interfaces [6,7]. Besides providing enhanced physical and chemical stability, these systems offer benefits such as lower toxicity, reduced cost, and the ability to recover particles [8].

The effectiveness of solid particles in stabilizing Pickering emulsions is directly related to their physicochemical characteristics, including size, morphology, wettability, and interaction with the oil and water phases. Nanoparticles and microparticles are particularly important because they offer high surface area and favorable interfacial behavior. In topical systems, properties such as surface polarity and particle size control also influence the formation of occlusive films, the skin retention, and the release of active ingredients [9]. Studies with cosmetic matrices demonstrate that silica-based Pickering emulsions can increase the deposition of active ingredients and improve the fixation of UV filters on the skin surface when compared to conventional emulsions [8].

Although inorganic particles, especially silica particles, alumina, and clay have been extensively investigated as Pickering emulsion stabilizers, concerns related to their safety and biocompatibility have encouraged the search for more sustainable alternatives [10,11]. In this context, polysaccharides with surfactant properties, such as pectin, gum Arabic, modified starches, chitin, chitosan, galactomannans, and cellulose, have gained prominence due to their biodegradability, biocompatibility, and interfacial adsorption capacity [12,13]. Although many macromolecules and biopolymers are widely recognized for their abundance, safety, and biodegradability, their practical use often depends on chemical modification steps to achieve the desired functional properties [14]. These additional processes may lead to increased energy consumption, higher costs, and the use of chemical reagents, thereby compromising the sustainability of these materials and limiting their application beyond the food sector. In comparison, nanocellulose stands out as an alternative more closely aligned with green principles [15].

Bacterial cellulose (BC) is a high-purity microbial polysaccharide characterized by a high crystallinity, high porosity, excellent water retention, and a mechanically strong three-dimensional nanofibrillar network [16–20]. Although it shares the same molecular formula as plant cellulose, it lacks hemicellulose and lignin and has highly ordered, hydrophilic microfibrils [21]. These features make its nanostructured particles effective stabilizers of Pickering emulsions thanks to their biocompatibility, sustainability, and large surface area, which promotes the formation of dense particulate barriers [22]. Among

these, the nanocrystals have an elongated shape that favors interfacial adsorption and oil/water stabilization [9]. Therefore, BC stands out as an alternative to plant cellulose in cosmetic, biomedical, and industrial applications because of its purity, crystallinity, and rheological properties [23]. Despite the extensive description of nanocrystals as effective emulsifiers [24–26], there are still few studies evaluating BC as a stabilizer for Pickering systems, especially in a nanofiber form [27,28].

Given these gaps, it is crucial to understand the interfacial behavior of BC in Pickering systems. This study compares oil/water emulsions stabilized by nanofibers and nanocrystals produced by acid hydrolysis using hydrochloric and sulfuric acids, respectively. After characterizing the structure of these particles, their effectiveness as stabilizers and their performance in formulating a moisturizing cream were assessed.

2. Materials and Methods

2.1. Production and Purification of Bacterial Cellulose

The *Komagataeibacter hansenii* UCP1619 strain deposited at the Center for Resources in Environmental Sciences (NPCIAMB) of the Catholic University of Pernambuco (Brazil) was used to produce bacterial cellulose (BC) membranes [29].

BC was produced by transferring 10% (*v*/*v*) of a pre-inoculum to a modified HS culture medium [30], which contained 1.5% glucose, 2.5% corn syrup, 0.27% Na_2HPO_4, and 0.15% citric acid, and had its pH adjusted to 5.0 [31]. The medium was sterilized in an autoclave at 125 °C for 15 min.

The culture was conducted under static conditions at 30 °C for 15 days. After this period, the BC formed was collected. Initial cleaning was performed by washing in running water, and purification was carried out by immersing the membranes in 0.1 M NaOH at 70 °C for 2 h. Subsequently, the membranes were washed with distilled water until the NaOH was completely removed, stored at 4 °C, and immersed in sterile distilled water.

2.2. Preparation of Bacterial Cellulose Fiber

The purified wet cellulose membranes were ground in a blender at 15,000 rpm for 1 min at room temperature. After centrifuging the suspensions at 3040× *g* for 10 min to remove any free water, the fibers were subjected to two different hydrolysis procedures, one using 2.5 M HCl at 70 °C and another using 60% (*w*/*w*) H_2SO_4 at 45 °C, both under magnetic stirring for 60 to 90 min, resulting in bacterial cellulose nanofibers (CNFs) and bacterial cellulose nanocrystals (CNCs), respectively [28,32]. After hydrolysis, the suspensions were washed with deionized water and centrifuged at 10,000× *g* to remove the acids.

2.3. Physicochemical Characterization of Hydrolyzed Fibers

2.3.1. Morphological Analysis

The morphologies of the nanofibers and nanocrystals in aqueous suspensions were examined by Transmission Electron Microscopy (TEM) using a JEM-1400 (JEOL, Tokyo, Japan) transmission electron microscope operating at 100 kV. Images were captured and processed using TEM-CENTER software (version 1.7.30.3157), and width and length were measured from individual particles [28].

2.3.2. Measurements of Droplet Size and Zeta Potential (ζ)

The zeta potential (ζ) was measured from the electrophoretic mobility of the dispersed particles, while the particle size distributions of the cellulose fibers were obtained by measuring dynamic light scattering (DLS) using a particle size analyzer (Particle Analyzer, Anton PAAR-Litesizer 500, Graz, Austria) equipped with Anton PAAR Kalliope Profes-

sional/2.34.3 software. Both tests were performed in triplicate, and the results are presented as average values at 25 °C [28].

2.3.3. Fourier Transform Infrared Spectroscopy (FTIR)

FTIR spectra of the fiber samples were obtained using an OPUS Vortex 70 spectrometer (Bruker, Billerica, MA, USA) in absorption mode, operating in the spectral range of 4000–400 cm^{-1} in ATR mode, with a resolution of 4 cm^{-1} and 16 scans (Platinum Attenuated Total Reflection, Bruker, Bremen, Germany) [28].

2.3.4. Contact Angle Measurement

The contact angle of the fibers was measured using FIJI ImageJ software (Java 8 64-bit version), considering a scale of 1 pixel = 1 mm. The fibers were prepared as films with a diameter of 13 mm and a thickness of 1–2 mm, which were molded in Petri dishes and left to dry at room temperature until a solid film was formed.

After drying, a drop of Milli-Q water (4 µL) was deposited onto the film surface using a high-precision injector. The image of the drop was captured by a high-speed video camera after 1 s, and the drop profile was solved numerically and fitted to the Laplace–Young equation [33]. Three measurements were performed for each sample.

2.4. Preparation of Pickering-Type Emulsions

Two sets of Pickering emulsion tests were performed using the CNFs and CNCs prepared from wet fibers. A phosphate-buffer solution (10 mM, pH 7.0) was used in both sets. The oils used were jojoba, grapeseed, and castor oil. The tests were performed in triplicate.

In the first set of tests, different fiber ratios (samples designated as FR) were evaluated. Oil/water emulsions were prepared in 10 mM phosphate buffer (pH 7.0) to achieve an oil/water ratio of 15% (v/v). A volume of 8.5 mL of a 10 mM phosphate-buffer solution (pH 7.0; aqueous phase) and 1.5 mL of the oily phase were used, totaling 10 mL for the dispersed system. Under these conditions, only the amount of nanofibers was varied to obtain final concentrations (w/v) of 0.01% (FR1), 0.03% (FR2), 0.05% (FR3), 0.07% (FR4), and 0.09% (FR5).

In the second set of tests, different oil proportions (samples designated as OR) were tested while keeping the nanofiber concentration constant at 0.05% (w/v), i.e., the total volume of the oil and buffer mixture was kept constant at 9.5 mL and the amount of fiber was set at 0.5 g, resulting in a system final volume of 10 mL. Thus, emulsions were prepared with different oil-to-buffer proportions (v/v): 5% (OR1), 10% (OR2), 15% (OR3), 20% (OR4), 25% (OR5), and 30% (OR6). All samples were homogenized in a vortex mixer (AP-56/1, Tecnal, Piracicaba, Brazil) for 1 min. The emulsification index (EI%), calculated as a percentage according to Cooper and Goldenberg [34], was assumed as an index of product stability.

2.5. Physicochemical Characterization of Emulsions

2.5.1. Interfacial Tension of Droplets

The interfacial tension of droplets was measured at 25 ± 0.5 °C using a digital tensiometer (Sigma 700, KSV, Helsinki, Finland), following the Du Nouy ring-pull method [35]. A 2:3 weight ratio of the oil phase to the aqueous phase was used for each sample, which was deposited in layers. The samples were prepared with the two fiber fractions (CNFs and CNCs) and with the selected oils and then left to stand for 30 min at 25 °C before each measurement. Each sample was analyzed in triplicate, and the results were expressed as the mean ± standard deviation.

2.5.2. Emulsion Stability

The ratios that ensured the best emulsification indices (fiber and oil and aqueous phase) were subjected to variations in pH (3, 7, and 11) and temperature (20, 60, and 100 °C for 30 min), in addition to mechanical action and a centrifugal force of 4000× *g* for 30 s to 5 min [36]. The stability of the emulsions was evaluated by visual inspection on the day of preparation and after 24 h and 7 days. The samples were stored at room temperature throughout the test period to allow for visual monitoring of possible physical changes. Emulsions that maintained stability under the evaluated factors were stored for 8 weeks.

2.5.3. Optical Microscopy of Emulsions

Images of the emulsions were captured using an Olen Fusi T1A optical microscope (São José dos Pinhais, Brazil) after sample preparation and after 60 days of storage [28]. Particle size measurements were obtained from 40× magnified images and analyzed using ImageJ software (National Institutes of Health (NIH), WI, USA). According to Mie's theory, the Sauter diameter, D_{32}, which is the area-weighted average diameter, was used to express particle size. This diameter was calculated according to the equation

$$D_{32} = \frac{\Sigma\, n_i\, d_i^3}{\Sigma\, n_i d_i^2} \quad (1)$$

where n_i is the number of particles with diameter d_i [37].

2.6. Cosmetic Formulation

The cellulose nanocrystals were purified by successively washing them with deionized water under vacuum filtration until a pH close to 4.0 was achieved in order to remove residues from the production process. Subsequently, using a methodology adapted from Wei et al. [38], the CNCs were subjected to additive-assisted drying using an ethanol–water solution (80% *v*/*v*) for 12 h and dried in an oven at 40 °C, resulting in a material with an approximate pH of 5.0. After preparation, the nanocrystals were stored at 4 °C.

The cosmetic formulation was a conditioning cream composed of deionized water (70–80%); vegetable oil (5–10%); glycerin (1–8%); bacterial cellulose nanocrystals (1–8%); emollient agents, namely, cetostearyl alcohol (1–10%), ceteareth-20 (1–10%), and PEG-7 glyceryl cocoate (1–10%%); and a preservative system based on phenoxyethanol (0.1–0.5%) and sorbate (0.1–0.5%).

Control formulations and formulations containing only CNCs, without PEG-7, were prepared to evaluate the influence of the fibers on the physicochemical properties and stability. In the control formulation and the PEG-7-free formulation, the volume corresponding to the absence of this component was compensated for by adding deionized water to maintain the same total volume of the formulation.

Prior to incorporation, the CNCs were rehydrated until a homogeneous, gel-like dispersion was obtained. The formulation components were then combined using conventional emulsification procedure, under controlled agitation, until a homogeneous and stable system was formed, followed by pH adjustment to the range suitable for the conditioners (4.5–5.0).

The samples were subjected to preliminary stability tests (centrifugation, moisture content determination, rheological analysis of apparent viscosity, and accelerated stability studies) at different temperatures (4 and 60 °C) for 7 days, with daily pH monitoring. These evaluations were limited to physicochemical stability and rheological behavior, and no quantitative sensory or conditioning performance assessments were conducted at this stage.

2.7. Statistical Analysis

All experiments were performed in independent replicates, and the results are shown as the mean ± standard deviation. The assessment and comparison of the systems were based on average values and variability.

3. Results and Discussion

3.1. Hydrolyzed Fibers

3.1.1. Fiber Morphology

The prepared celluloses showed similar characteristics to those produced by Galdino et al. [39] using the same medium and conditions. Static bacterial cellulose cultures with a working volume of 3 L per batch yielded about 400 g of wet milled cellulose. After purification and acid hydrolysis, the mass dropped to around 300 g (wet basis). Subsequent washing and additive-assisted drying steps resulted in roughly 6–7 g of dry cellulose nanofibers (CNFs). This significant reduction in mass is due to the high moisture content, which indicates that the bacterial cellulose contained approximately 97% water in its native state. Therefore, removing free and bound water during processing caused a substantial decrease in the final dry fiber yield while maintaining the cellulose solid fraction.

The fibers hydrolyzed with HCl (Figure 1D) showed perceptible opacity and granulometry as macroscopic characteristics, indicating partial hydrolysis of the cellulose matrix. In contrast, the samples hydrolyzed with H_2SO_4 (Figure 1E) exhibited higher transparency, increased surface brightness, and reduced granulometry, suggesting a more effective disruption of the amorphous regions of cellulose.

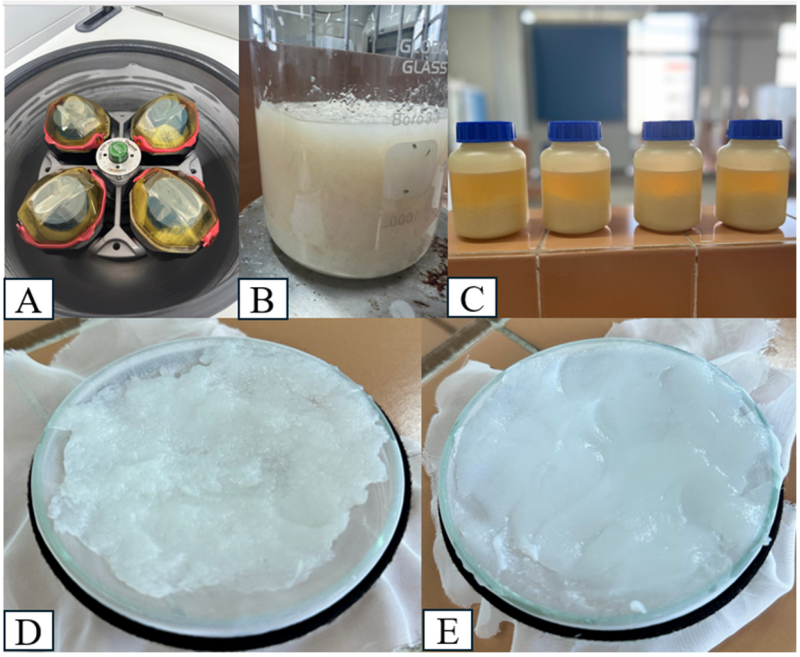

Figure 1. Preparation and chemical hydrolysis of bacterial cellulose fibers. (**A**) Centrifugation step used to remove excess water from bacterial cellulose; (**B**) visual appearance of the bacterial cellulose during the acid hydrolysis process; (**C**) release of free water from the bacterial cellulose fiber; (**D**) bacterial cellulose fiber hydrolyzed with HCl; (**E**) bacterial cellulose fiber hydrolyzed with H_2SO_4.

The classification of the hydrolyzed materials was based on the extent of acid-induced depolymerization and their resulting structural features. Hydrolysis with HCl resulted in partial cleavage of cellulose chains, producing shortened yet still predominantly polymeric and fibrillar structures, referred to here as cellulose nanofibers (CNFs). In contrast,

H_2SO_4 hydrolysis disrupted amorphous regions more effectively, producing mainly crystalline, rod-shaped domains characteristic of cellulose nanocrystals (CNCs). This naming aligns with the related literature and was confirmed by the microscopic analyses described below.

Acid hydrolysis of BC yielded distinct structures depending on the acid used, as observed in the Transmission Electron Microscopy (TEM) micrographs (Figure 2). Acid hydrolysis with HCl led to the formation of nanofibers (CNFs) with an elongated, intertwined morphology, resulting in a disorganized three-dimensional network and greater heterogeneity in diameter and length (Figure 2A). This structure shows agglomerated regions and amorphous remnants, which are characteristic of networks without charged functional groups, which are absent due to the non-sulfating character of HCl [40,41].

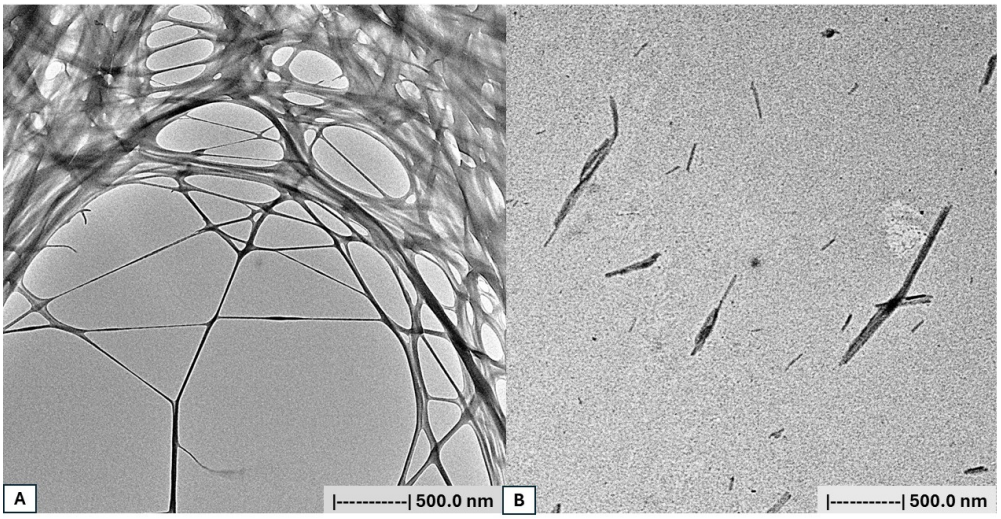

Figure 2. Transmission Electron Microscopy (TEM) images of bacterial cellulose nanostructures. (**A**) Bacterial cellulose nanofibers (CNFs) displaying an interconnected fibrillar network; (**B**) bacterial cellulose nanocrystals (CNCs) exhibiting a rod-like shape. Scale bar: 500 nm.

Conversely, hydrolysis with H_2SO_4 produced short, stiff, and well-defined nanocrystals (CNCs) with a uniform size and high dispersion (Figure 2B). This shape indicates the selective removal of amorphous areas and the preservation of crystalline regions, which are typical of nanocrystals. Additionally, the process introduces sulfate functional groups ($-OSO_3^-$) on the surface, increasing surface charge, promoting electrostatic repulsion, and leading to greater colloidal stability, as shown by the reduced tendency to agglomerate [28].

3.1.2. Colloidal Stability

Zeta potential was determined as an indicative parameter of the colloidal stability of the particulate systems, which were also characterized in terms of hydrodynamic size, polydispersity index, conductivity, and transmittance; the values are listed in Table 1. The CNFs showed an average zeta potential value of +21.9 mV, indicating moderate electrostatic stability, while the CNCs showed an average value of −33.9 mV, indicating high electrostatic stability. This difference can be attributed to the introduction of sulfonic groups ($-SO_3-$) on the surface of the cellulose fiber.

Pang et al. [42], in their study on vegetable cellulose nanocrystals hydrolyzed with 64% sulfuric acid, reported a zeta potential of approximately −33 mV, a value comparable with the results obtained in the present study. Pinto et al. [28] reported zeta potentials of −47 mV for nanofibers prepared by oxidation (TEMPO/NaOCl/NaBr) and −50 mV for nanocrystals prepared by hydrolysis (H_2SO_4) of BC produced in synthetic HS medium; both values indicate high colloidal stability. Hydrolysis with HCl did not significantly alter

the fiber surface, which maintained a low surface charge and low electrostatic repulsion. As repulsion is important for avoiding coalescence in Pickering emulsions, this results in lower emulsion stability.

Table 1. Zeta potential, hydrodynamic size, polydispersity, conductivity, and transmittance of bacterial cellulose nanofibers (CNFs) and bacterial cellulose nanocrystals (CNCs).

Parameter	CNFs	CNCs
Zeta potential (mV)	21.9	−33.9
Hydrodynamic size (nm)	525.00	848.30
Polydispersity index (PDI, %)	28.20	25.50
Conductivity (mS/cm)	4.98	0.21
Transmittance (%)	85.50	87.20

The CNFs and CNCs showed hydrodynamic sizes of approximately 525.0 nm and 848.3 nm, respectively. The smaller size of the nanofibers may indicate a greater dispersion of fibers in the continuous phase; however, this does not necessarily reflect greater system stability. Conversely, the larger apparent diameter of the nanocrystals could be related to the formation of organized aggregates. Pinto et al. [28] measured the hydrodynamic diameters of fibers hydrolyzed with HCl (25–146 nm) and H_2SO_4 (133–870 nm), which were significantly different from those observed in this study for CNFs but not for CNCs. Despite representing larger particles, these values were accompanied by a high negative zeta potential, which may offset the size increase and suggest the formation of a thicker and possibly more stable interfacial coating around oil droplets. In Pickering emulsions, the particle size must be sufficient to cover the interface and form an effective physical barrier; thus, slightly larger particles, such as those seen in the CNC samples, can provide greater strength to the interfacial structure.

The polydispersity index (PDI), which indicates the uniformity of the particle size distribution in suspension, showed high values in both samples, characterizing polydisperse systems [43]. Values of 28.2% and 25.5% were observed for the CNFs and CNCs, respectively, with the latter being slightly more homogeneous. The high polydispersity can be attributed to the intrinsically irregular morphology of BC fibers and the possible presence of agglomerates. Even so, the lower size variation observed for the CNCs suggests a more controlled dispersion, possibly favored by the negative charge of the sulfated surface, which hinders disordered agglomeration among fibers.

The electrical conductivity also varied significantly between the dispersions, with the nanofiber and nanocrystal samples showing values of 4.98 and 0.211 mS/cm, respectively. This difference may be due to residual free ions from acid hydrolysis. The higher conductivity of the CNFs could indicate the presence of leftover chloride ions (Cl^-), which can negatively impact system stability and reduce electrostatic repulsion efficiency. The low conductivity of the CNCs suggests that the charged (sulfonic) groups are strongly attached to the cellulose surface, supporting stable and effective colloidal stabilization [44].

The optical transmittance was similar in both samples, with a slightly higher value for the CNCs (87.2%) over the CNFs (85.5%). Despite this small difference, this behavior may indicate lower turbidity in the system containing sulfated BC, which may be associated with partial sedimentation of larger particles or the formation of a more stable interfacial structure. A similar behavior was reported by Alade et al. [45] in cellulose-based systems. In Pickering emulsions, high transmittance values suggest a lower quantity of free particles in the continuous phase, which is favorable for the adsorption of these particles at the oil/water interface.

3.1.3. Structural Characterization of Fibers

The hydrolyzed BC samples were characterized by Fourier transform infrared spectroscopy (FTIR) (Figure 3), which allowed for the identification of the main functional groups characteristic of cellulose. In both samples, a broad band was observed in the wavenumber region of 3200 to 3400 cm^{-1}, ascribed to the stretching of hydroxyl groups (OH^-), which confirms the presence of hydrogen bonds; however, in the CNF sample, this band showed greater intensity and a slight shift, suggesting greater moisture retention and a less crystalline structure.

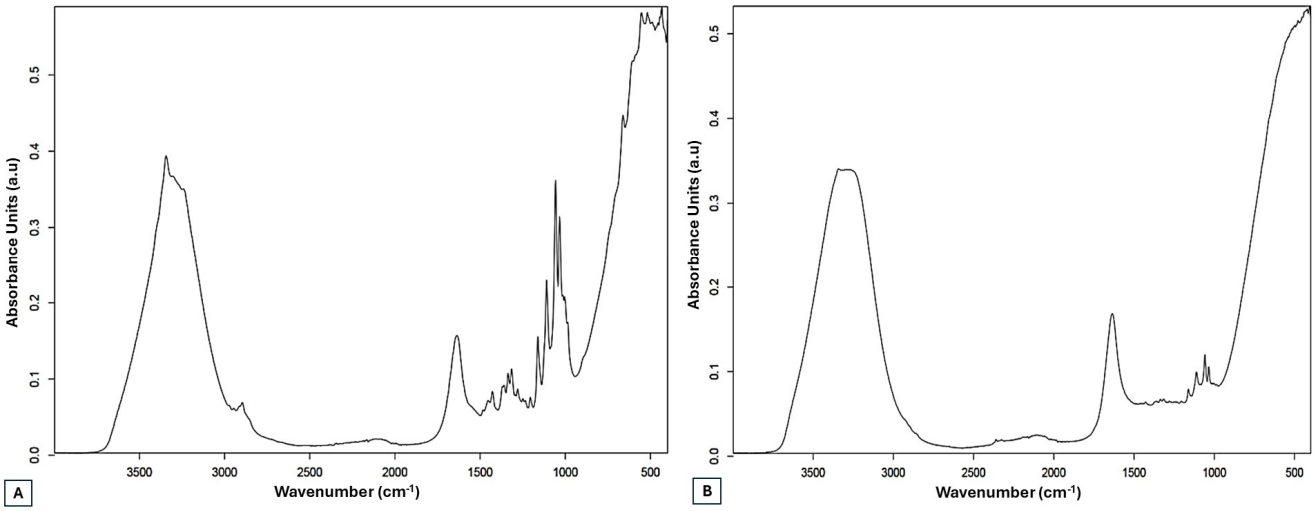

Figure 3. FTIR spectra of (**A**) bacterial cellulose nanofibers (CNFs) and (**B**) bacterial cellulose nanocrystals (CNCs).

The bands at ~2900 cm^{-1} and ~1640 cm^{-1}, related to C-H bonds and absorbed water, reinforce this interpretation. In the CNC spectrum, the sharper CH_2 vibrations in the 1430–1370 cm^{-1} region indicate greater structural order, while the better-defined bands in the 1160–1050 cm^{-1} region, corresponding to C-O-C and C-O bonds, point to a higher crystallization index, consistent with the formation of nanocrystals via sulfuric hydrolysis. The region below 1000 cm^{-1} in the CNF spectrum exhibits greater spectral complexity, possibly resulting from a less organized matrix. In general, CNCs show greater crystallinity, favoring the formation of nanocrystals, while CNFs maintain more amorphous characteristics, with a predominance of nanofibers [28,42,46].

From the perspective of applications in Pickering emulsions, CNCs hydrolyzed with H_2SO_4 appear to be better suited. This is because the nanocrystals obtained through sulfuric acid hydrolysis have sulfate groups on their surface, which confer a negative charge and promote stabilization via electrostatic repulsion and steric barriers among oil–water droplets [47]. Additionally, nanocrystals with a slightly hydrophobic surface can interact efficiently with oil/water interfaces, forming stable emulsions [48]. Recent studies have shown that sulfated nanocrystals effectively stabilize Pickering emulsions, demonstrating high coalescence stability and sensitivity to pH and ionic strength. CNFs, on the other hand, are primarily composed of amorphous nanofibers and have less capacity for interfacial stabilization due to a lack of charged groups and lower crystalline rigidity [47,49].

3.1.4. Fiber Hydrophilicity

The CNF and CNC samples showed contact angles of 31.8 and 50.17°, indicating more hydrophilic and more hydrophobic characteristics, respectively. While the CNFs hydrolyzed with HCl showed lower wettability, the CNCs obtained by hydrolysis with H_2SO_4 were closer to having a constant wettability (90°). Pinto et al. [28] reported contact

angles of 30° and 31° for cellulose nanofibers and nanocrystals, respectively, which characterizes them as hydrophilic materials. The value obtained in the present study for the CNFs agrees with that reported by those authors, while the one obtained for the CNCs was much higher, indicating a tendency towards greater wettability and lower affinity with the aqueous phase.

Measuring the contact angle is essential for identifying whether a film is hydrophilic or hydrophobic. A key factor in the stability of Pickering emulsions is the wettability of the particles at the oil–water interface [50,51]. If the contact angle is less than 90°, the particles are considered hydrophilic or moderately hydrophilic because the stabilizers dissolve more easily in the emulsion, offering greater stability at the oil–water interface. Conversely, when the particles have a contact angle greater than 90°, the film tends to prevent liquid spreading, indicating a hydrophobic surface. A balance of wettable particles in the oil–water phases is necessary; generally, the closer the angle is to 90°, the better the balance between hydrophilicity and hydrophobicity, which enhances stability [52,53].

3.1.5. Interfacial Tension of Droplets

The average interfacial tension values of jojoba, castor, and grape seed vegetable oils were 32.62, 34.79, and 32.00 mN/m, respectively. The addition of hydrolyzed fibers led to distinct reductions in these values, highlighting the influence of hydrolysis type on the particles' interfacial activity. The CNCs showed a greater capacity for reducing interfacial tension, reaching 27.43 mN/m in jojoba oil and 29.80 mN/m in castor oil, indicating greater interfacial efficiency compared to the CNFs, whose values were 31.44 and 40.19 mN/m, respectively. In grape seed oil, the variations were less pronounced, with values close to the initial ones: 32.42 mN/m with CNFs and 32.99 mN/m with CNCs.

The reduction in interfacial tension observed in the CNC samples indicates the formation of particles with a higher capacity for adsorption and stabilization at the oil/water interface, resulting in more stable emulsions. According to Pinto et al. [28] and Carvalho-Guimarães et al. [54], lower interfacial tension values are linked to increased resistance of the droplets to coalescence, thereby enhancing emulsion stability. Conversely, higher values signify reduced interfacial resistance and a greater likelihood of droplet rupture and system destabilization.

Hydrolysis with HCl tends to preserve cellulose's more amorphous structure, resulting in a smaller effect on interfacial tension. Conversely, hydrolysis with H_2SO_4 promotes the formation of cellulose nanocrystals, which have a larger specific surface area, and enhances particle adsorption at the interface, thereby decreasing interfacial tension.

3.2. Pickering Emulsions

3.2.1. Bacterial Cellulose Nanofibers (CNFs)

In the formulations prepared with different fiber ratios (designated as FR), regardless of the type of oil used (jojoba, castor, or grape seed oil), a consistent behavior was observed: an increase in emulsion stability as the cellulose fiber mass increased. For the formulations with jojoba oil, the stability ranged from approximately 33% to 80% on the first day and from 28% to 80% after one week, except for sample FR1, which showed an 18% reduction in the first 24 h. Similar results were obtained for the formulations with castor oil, with average values ranging from 26% to 93% on the day of production and from 18% to 80% after 7 days, reinforcing the positive effect of fiber mass. With grape seed oil, a similar trend was observed, with values between 25% and 90% on the initial day and between 25% and 85% at the end of the test, though with greater variability among replicates. These results consistently indicate that, with all three oils, increasing the nanofiber

concentration promotes the stabilization of Pickering emulsions over time, although the level of stability varies depending on the type of oil phase.

In the formulations prepared with different oil ratios (designated as OR), the three oils exhibited a more uniform behavior characterized by initial average values close to 50% stability and a smaller effect of the oil type on time variations. For the formulations with jojoba oil, the samples with a lower oil volume showed greater stability, while samples OR5 and OR6 experienced a reduction from 70% and 63% to values near 53% by the end of the experimental period. The formulations with castor oil displayed average values between 25% and 75% on the first day and between 28% and 50% after 7 days, with sample OR2 standing out for maintaining a steady 50% stability throughout the experiment. Similarly, with grape seed oil, the average values stayed close to 50% throughout the week, with no significant changes. Overall, these results show that, in OR formulations, the volume of oil influences stability more than its chemical nature, with smaller volumes promoting stability and reducing variation among replicates (Tables S1–S3).

The changes in the emulsification indices of the Pickering emulsions using CNFs and phosphate-buffer solutions of jojoba, castor, and grape seed oils over a period of 7 days are listed in Table 2.

Table 2. Emulsification index (%) of samples prepared in triplicate with different fiber (FR) and oil (OR) ratios. The emulsion tests were performed over 7 days using jojoba, castor, and grape seed oils and nanofibers prepared by hydrolysis with HCl. Data are presented as the mean ± standard deviation. FR samples: oil/water emulsions in a 15% (v/v) ratio prepared with 10 mM phosphate buffer containing nanofiber concentrations (w/v) of 0.01% (FR1), 0.03% (FR2), 0.05% (FR3), 0.07% (FR4), and 0.09% (FR5). OR samples: 0.05% (w/v) nanofiber emulsions prepared with 10 mM phosphate buffer containing oil-in-water (v/v) concentrations of 5% (OR1), 10% (OR2), 15% (OR3), 20% (OR4), 25% (OR5), and 30% (OR6).

	Emulsification Index (%)		
	Jojoba Oil	**Castor Oil**	**Grape Seed Oil**
FR			
FR1	28.33 ± 5.77	18.33 ± 2,89	25.00 ± 0.00
FR2	38.33 ± 5.77	36.67 ± 5,77	31.67 ± 7.64
FR3	48.33 ± 2.89	50.00 ± 0.00	50.00 ± 0.00
FR4	68.33 ± 2.89	60.00 ± 0.00	60.00 ± 0.00
FR5	80.00 ± 0.00	80.00 ± 0.00	85.00 ± 0.00
OR			
OR1	51.67 ± 2.89	50.00 ± 0.00	50.00 ± 0.00
OR2	51.67 ± 2.89	50.00 ± 0.00	45.00 ± 0.00
OR3	48.33 ± 2.89	50.00 ± 0.00	46.67 ± 5.77
OR4	50.00 ± 0.00	28.33 ± 2.89	50.00 ± 0.00
OR5	53.33 ± 2.89	30.00 ± 0.00	50.00 ± 0.00
OR6	53.33 ± 2.89	36.67 ± 5.77	50.00 ± 0.00

The results collected after the 7-day experiments show that the FR samples with the three oils showed similar behaviors. The emulsification index varied between 28 and 80% for jojoba oil, between 18 and 80% for castor oil, and between 25 and 85% for grape seed oil, confirming that the emulsion stability increases proportionally with the mass of BC nanofibers. The performance of the FR5 sample stands out in this regard. For standard deviation, a value closer to zero indicates less variation between replicates and, therefore, greater consistency of data. The standard deviation results for the grape seed oil formulation were the most satisfactory, since most samples showed negligible standard deviations.

The OR formulations with the three oils showed similar behaviors, with average values close to 50%. These findings indicate that, under the tested conditions, the volume

of oil in the emulsion has a limited influence on stability and can be considered almost negligible. However, the standard deviation results for the grape seed oil formulations also stand out as they were even lower, with an average variation of around 5%, indicating greater uniformity and stability.

3.2.2. Bacterial Cellulose Nanocrystals (CNCs)

In the FR formulations with BC nanocrystals and the three oils, a consistent pattern was observed. For the formulations with jojoba oil, the initial values ranged from 71% to 100%, which decreased to between 55% and 93% by the end of the experiment; sample FR5 showed the greatest stability. With castor oil, a consistently high initial stability of 100% was seen, followed by fluctuations between 25% and 98% after 7 days, indicating a trend of increasing stability as the nanocrystal amount increased. Similarly, for the formulations with grape seed oil, the samples started with values between 80% and 100%, and at the end of the experiment, the values were between 25% and 100%, with stability improving as the nanocrystal concentration increased. The only notable exception was sample FR1, which experienced a sudden drop from 81.67% to 2% within the first 24 h. Overall, these findings suggest that higher concentrations of nanocrystals in FR formulations significantly improve the stability of Pickering emulsions, although some samples showed high variations in the initial values.

In the OR formulations, a more consistent pattern was observed, characterized by high initial stabilities, often close to or at 100%, followed by a decline linked to increasing oil volume. For the formulations with jojoba oil, the values ranged from 91 to 100% initially, which decreased to 41 to 97% by the end of the period; OR1 showed the greatest consistency and OR2 displayed high variability among replicates. Similar results were obtained with castor oil, with values near 100% in the first 24 h, which then decreasing as the oil ratio increased; OR4 experienced a 50% reduction over 7 days. For the formulations with grape seed oil, the performance was even more notable, with all samples starting at 100% and staying above 90% until the experiment's end. Notably, OR1 remained completely stable throughout. Overall, these results suggest that in OR formulations, oil volume significantly influences stability, with smaller volumes yielding more consistent results and higher stability, regardless of the oil type used (Tables S4–S6).

The results obtained throughout the week of observation for Pickering emulsions using CNCs and phosphate-buffer solutions of jojoba, castor, and grape seed oils are listed in Table 3.

Analyzing the results of samples containing fibers treated with sulfuric acid and the three oils, it was observed that the FR formulations with jojoba oil showed average emulsification index values ranging from 55% to 93%, those with castor oil showed values ranging from 25% to 98%, and those with grape seed oil showed values ranging from 25% to 100%. Overall, emulsion stability increased with fiber content. However, the FR2 sample with jojoba oil stood out by showing a slight decrease in stability compared to FR1, which remained more stable than the FR1 samples with castor and grape seed oils.

Most of the OR formulations showed stability values above 80%. However, the formulations with jojoba oil yielded worse results than those with grape seed oil, which showed stability values above 90% and very low standard deviations. Grape seed oil showed the best performance among the three oils in both experiments.

The results from the formulations with two cellulosic materials indicate that they exhibited the same behavior, but the nanocrystals performed better in both experiments and with the three vegetable oils studied. Indeed, samples FR4, FR5, OR1, and OR2 containing CNCs showed emulsification index values greater than 80% with

all the tested oils. In contrast, the nanofiber samples showed values between 50 and 60%, except for sample FR5, which achieved 80% stability in all formulations.

Table 3. Emulsification index (%) of samples prepared in triplicate with different fiber (FR) and oil (OR) ratios. The emulsion tests were performed over 7 days with jojoba, castor, and grape seed oils and nanocrystals obtained by hydrolysis with H_2SO_4. Data are presented as the mean ± standard deviation. FR samples: oil/water emulsions in a 15% (*v*/*v*) ratio prepared with 10 mM phosphate buffer containing nanofiber concentrations (*w*/*v*) of 0.01% (FR1), 0.03% (FR2), 0.05% (FR3), 0.07% (FR4), and 0.09% (FR5). OR samples: 0.05% (*w*/*v*) nanocrystal emulsions prepared with 10 mM phosphate buffer containing oil-in-water (*v*/*v*) concentrations of 5% (OR1), 10% (OR2), 15% (OR3), 20% (OR4), 25% (OR5), and 30% (OR6).

	Emulsification Index (%)		
	Jojoba Oil	**Castor Oil**	**Grape Seed Oil**
FR			
FR1	60.00 ± 17.32	25.00 ± 0.00	25.00 ± 0.00
FR2	55.00 ± 0.00	68.33 ± 7.64	41.67 ± 7.64
FR3	61.67 ± 7.64	73.33 ± 2.89	81.67 ± 2.89
FR4	85.00 ± 0.00	88.33 ± 2.89	91.67 ± 5.77
FR5	93.33 ± 2.89	98.33 ± 2.89	100.00 ± 0.00
OR			
OR1	97.00 ± 1.73	90.00 ± 0.00	100.00 ± 0.00
OR2	86.00 ± 10.39	80.00 ± 5.00	98.00 ± 0.00
OR3	70.00 ± 0.00	85.00 ± 0.00	96.00 ± 1.73
OR4	53.33 ± 5.77	53.33 ± 5.77	95.67 ± 1.15
OR5	55.00 ± 5.00	68.33 ± 7.64	96.67 ± 1.53
OR6	41.67 ± 7.64	85.00 ± 0.00	96.00 ± 1.73

Ferreira et al. [46] investigated vegetable cellulose nanofibers in Pickering emulsions with buriti oil observed that high concentrations of nanofibers played a key role in maintaining the stability of the oil/water emulsions over 30 days of storage. Tan et al. [55], when evaluating Pickering emulsions stabilized by BC nanofibers using rapeseed (canola) oil as the oil phase, observed that the emulsification index tended to decrease faster over a period of 14 days as the oil fraction increased. This behavior contrasts with the emulsions formulated with jojoba, castor, and grape seed oils in this study, where the same trends based on changes in the dispersed phase were not observed. The FR and OR formulations with the best results were used in the subsequent stability and optical microscopy tests.

The observed differences in the stability of emulsions made with jojoba oil, castor oil, and grape seed oil can be explained by the unique physicochemical properties of these oils, especially their viscosity, polarity, and fatty acid composition. Castor oil shows higher viscosity and polarity because of its high content of ricinoleic acid, a hydroxylated fatty acid that encourages stronger intermolecular interactions. These traits decrease droplet movement and help form a more durable interfacial barrier, which slows down coalescence and creaming processes [56].

In contrast, grape seed oil mainly consists of triacylglycerols rich in polyunsaturated fatty acids, especially linoleic acid, which leads to lower molecular packing and decreased viscosity of the oil phase. This increased droplet mobility can weaken the efficiency of the interfacial barrier created by the stabilizing particles, promoting instability during storage [57].

Jojoba oil is mainly composed of long-chain wax esters and shows rheological behaviors and a polarity between those of the other oils. This unique molecular structure may affect oil–water interfacial organization and the anchoring of stabilizing particles, resulting in emulsions with intermediate stability [58].

3.2.3. Effects of pH, Temperature, and Storage Time

In the CNF-containing PF formulations, pH had a decisive influence on emulsifying performance and system stability depending on the oil type. The jojoba oil systems at pH 7 and 11 showed similar behaviors, stabilizing at around 50% after 7 days, although both showed a sharp decline within the first 24 h, indicating an initially insufficient interfacial coverage to prevent coalescence. At pH 3, a continuous loss of stability was observed, suggesting that, in this specific system, CNF protonation was not enough to offset the lower interfacial affinity with jojoba oil. Conversely, using castor oil at pH 3 resulted in the best performance across all oils, maintaining about 90% stability throughout the experimental period, likely due to reduced electrostatic repulsion between protonated fibrils and the formation of a more cohesive, resistant interfacial barrier [59,60]. pH 7 yielded moderate stability (around 60%), reflecting a less favorable balance between interfacial organization and repulsive forces, while pH 11 caused a rapid loss of stability on the first day, showing the negative impact of excess negative charge on fiber–interface interactions. With grape seed oil, greater stability was observed at pH 7, with a moderate decrease from 75% to 65%, indicating that neutral conditions promoted more balanced interfacial adsorption. At pH 3, there was a more prominent initial drop followed by stabilization, while at pH 11, the system displayed low efficiency from the start without recovery, confirming the limitations caused by high electrostatic repulsion in an alkaline medium.

In the OR formulations, although the influence of pH was also evident, a general trend of lower final stability was observed, which was associated with a lower fiber concentration available for interface stabilization. For the jojoba oil formulations, at a pH of 3, constant stability around 50% was observed, suggesting that CNF protonation favors interfacial adsorption even in diluted systems; in contrast, the systems at pH 7 and 11, despite showing an initial value of 100%, suffered a rapid collapse with a reduction to about 30%, which indicates that the amount of fiber was not sufficient to sustain a continuous interfacial barrier over time. In the case of castor oil, neutral conditions ensured greater consistency, with a small drop from 80 to 70%, reflecting a balance between repulsion and interfacial affinity, while at pH 11, after an initial value of 100%, there was an abrupt drop, reinforcing the incompatibility of the alkaline medium with CNF stabilization. At pH 3, although the system showed good initial performance, it exhibited lower stability than that observed in the FR formulations, highlighting the role of fiber concentration in maintaining the emulsion. For the systems containing grape seed oil, both pH 3 and pH 7 resulted in low final stability values (30–40%), while at pH 11, despite high initial formation, rapid system degradation occurred, confirming that the increase in the negative charge of CNF compromises the formation of an efficient interfacial layer, especially under low solid fraction conditions (Table S7).

In the CNF-based FR formulations, the stability of the Pickering emulsions was also influenced by temperature, with different responses depending on the oil type. With jojoba oil, the FR5 formulation demonstrated high thermal resistance, maintaining about 90% stability at 20 °C and between 80 and 90% stability even after exposure to 60 °C and 100 °C, indicating that the interfacial structure remained functional despite increased molecular mobility. In the case of castor oil, better performance was observed at 20 °C, with the stability close to 100% in the first 24 h and holding at 98% after 7 days. However, increasing the temperature caused a steady decrease in stability, with a sharp decline on the first day at 60 °C and an immediate loss at 100 °C, followed by stabilization at lower levels. This suggests heating compromised the initial integrity of the system and limited its ability to reorganize afterward [61]. With grape seed oil, the FR5 formulation showed moderate stability at 20 °C and 60 °C, decreasing to about 50% stability after 24 h. At 100 °C, it exhibited better performance, maintaining roughly 75% stability throughout

the entire experiment, demonstrating a higher tolerance to more severe thermal disturbances. Overall, these results indicate that the FR formulations are more stable at low and intermediate temperatures, except for those with grape seed oil, which showed good thermal resistance even at 100 °C.

In the OR formulations, the temperature response was more heterogeneous and strongly dependent on the type of oil. For those with jojoba oil, stability remained limited to approximately 50% at 20 and 60 °C, while at 100 °C, there was an abrupt drop in the first 24 h and it remained low until the end of the test, reflecting greater sensitivity of the system to heating. In contrast, a different behavior was observed for the formulations with castor oil, which showed a progressive increase in stability at 20 °C throughout the first day and subsequent maintenance of this level, while at 60 °C, the system stabilized at around 50%. Notably, at 100 °C, the emulsion maintained approximately 70% stability, indicating that, under this specific condition, heating resulted in more efficient structural rearrangements after cooling. For the formulations with grape seed oil, stability remained low and practically constant at 20 and 100 °C; however, at 60 °C, the system showed high initial stability, followed by a slight reduction and subsequent maintenance, suggesting that intermediate temperatures temporarily favor the organization of the system even under conditions of lower fiber content (Table S8).

Table S9 shows the behavior of Pickering emulsions formulated with CNCs at different pH values (3, 7, and 11), using jojoba, castor, and grape seed oils as the oil phase. The FR5 formulations showed superior performance in acidic media with all evaluated oils, demonstrating that the rigid and highly crystalline nature of CNCs promotes interfacial organization under conditions of lower electrostatic repulsion [59]. For the formulations with jojoba oil, the emulsion maintained 100% stability at pH 3 throughout the 7 days, while at pH 7, there was a gradual reduction to approximately 80%, suggesting a partial loss of interfacial efficiency; at pH 11, the instability was accentuated, dropping to about 40% at the end of the experimental period, which is consistent with the reduced ability of excessively charged CNCs to form continuous layers. Similar behavior was observed using castor oil, with total stability observed at pH 3, a slight reduction at pH 7 (reaching 95% after 7 days), and a more pronounced loss at pH 11 (reaching approximately 60%), indicating that, even in intrinsically more compatible systems, the alkaline medium compromises the interfacial functionality of CNCs. The FR5 formulations with grape seed oil also showed greater stability at pH 3, maintaining approximately 90% stability until the seventh day, while at pH 7 and 11, there were more significant declines, reaching approximately 65 and 60%, respectively, reflecting the greater sensitivity of this system to variations in the surface charge of crystalline particles.

In the OR1 formulations, the same general pattern was maintained, but with a more sensitive response to pH variations, especially in neutral and alkaline media, where a lower particle concentration limited the CNCs' ability to sustain the interface over time. For the formulation with jojoba oil, stability remained high at pH 3, reaching about 95% after 7 days, while at pH 7, there was a sharp drop, reaching around 55% at the end of the test; at pH 11, instability occurred immediately, with a reduction to approximately 40% within the first 24 h. The formulation with castor oil again stood out for its superior performance in acidic media, maintaining 100% stability at pH 3, with a moderate decrease at pH 7 to about 85% after 7 days; however, at pH 11, a significant drop occurred on the first day, reaching about 55%, highlighting the low tolerance of CNCs in alkaline environments when the solid fraction is reduced. The OR1 emulsions with grape seed oil followed the same trend, showing good stability at pH 3 (around 90% after 7 days), moderate stability at pH 7 (~80%), and significant loss at pH 11 (~60%), indicating that, in less concentrated

systems, the high rigidity and crystallinity of CNCs make their interfacial efficiency highly dependent on acidic conditions.

According to the results in Table S10, the FR5 Pickering emulsions formulated with CNCs with all tested oils showed similar thermal behaviors, demonstrating strong resistance to coalescence even under heat stress. For jojoba oil, the initial stability was 100%, with slight decreases over seven days, reaching 85% at 20 °C, 90% at 60 °C, and 87% at 100 °C. This indicates that higher particle concentrations helped maintain the interfacial structure despite rising temperatures. With castor oil, stability remained near the maximum under all thermal conditions, staying above 98% at 20 and 60 °C and only slightly dropping to 95% at 100 °C. These results, which reflect the best performance among the systems tested, highlight the strong compatibility between the oil and the interfacial network created by the CNCs. The emulsion with grape seed oil also showed excellent initial stability, with moderate decreases during the test period, reaching 90% at 20 and 60 °C and 87% at 100 °C. These findings reinforce the robustness of the FR5 formulations against temperature changes.

The OR1 emulsions showed similarly high initial stability but were more sensitive to temperature changes compared to the FR5 formulations. This is due to the lower particle concentration affecting the system's structural strength. For the formulation with jojoba oil, the initial stability was 100%, but it gradually decreased to 85% at 20 °C and 80% at 60 °C, with a more significant drop to 55% at 100 °C after 7 days, indicating higher vulnerability to interfacial loss under intense heating. The formulation with castor oil performed better overall, maintaining 100% stability at 20 °C, which reduced to 75% at 60 °C, and stayed at 85% at 100 °C, showing excellent thermal resistance even with a lower particle content. The formulation with grape seed oil started with 100% stability at 20 °C, which decreased to 85% by the end of the testing period. At 60 and 100 °C, the final values stayed around 80%, signifying good thermal tolerance despite the smaller solid fraction. Overall, these findings reveal that the thermal stability of Pickering emulsions with CNCs is heavily affected by particle concentration and oil type, with castor oil—especially in the FR5 formulation—being the most effective for applications needing stability across a wide temperature range.

Zhang et al. [62] studied the stability of Pickering emulsions made with vegetable particles under different pH and temperature conditions and showed that a pH of 5 produced the best performance, with higher resistance to coalescence. Under acidic conditions (pH 3), the emulsion quickly deteriorated, while at pH levels between 7 and 11, stability was maintained, though with signs of gradual instability over time [62]. This pattern is similar to what was observed in the current study with the three tested oils: at pH 3, the emulsions lost stability more rapidly, while at pH 7 and 11, the deterioration was slower, emphasizing the importance of using a medium with a pH close to neutral. Regarding the thermal aspect, Zhang et al. [62] reported that the emulsions maintained stability after exposure to 50 °C for 4 weeks, with no significant changes in droplet size or distribution. In contrast, in the present work, more severe conditions (60 and 100 °C) were used, revealing different resistance behaviors: while CNC-stabilized emulsions remained highly stable up to 100 °C, the CNF-stabilized ones experienced notable losses, underscoring the fragility of these fibers under thermal stress. This work emphasizes the stability limits under extreme conditions, which are vital for high-temperature applications.

After 60 days of storage, the Pickering emulsions showed distinct stability behaviors depending on the type of cellulose and vegetable oil used (Table 4). The CNC-based formulations exhibited high colloidal stability, with the values for samples FR5 and OR1 ranging from 95 to 100%, regardless of the oil type. These results indicate that even after two months, the emulsions containing CNCs retained almost the entire emulsified phase,

with no significant separation between phases, demonstrating the formation of a solid interface resistant to coalescence. This suggests they can form more stable systems in the long term due to their highly crystalline structure, higher surface charge, and ability to create rigid, homogeneous interfacial layers.

Table 4. Storage stability (%) of Pickering emulsions formulated with bacterial cellulose nanofibers (CNFs) and bacterial cellulose nanocrystals (CNCs) and jojoba, castor, and grape seed oils after 2 months. FR5 samples: 15% (*v*/*v*) oil/water emulsion prepared with 10 mM phosphate buffer containing 0.09% nanofibers. OR1 samples: 0.05% (*w*/*v*) nanocrystal emulsion prepared in 10 mM phosphate buffer containing 5% (*v*/*v*) oil.

Oil	Nanoparticle	FR5 (%)	OR1 (%)
Jojoba oil	CNF	35	25
	CNC	98	98
Castor oil	CNF	60	30
	CNC	95	98
Grape seed oil	CNF	35	25
	CNC	100	98

In contrast, the emulsions prepared with the CNFs showed a significant reduction in stability, with values below 60% for the FR5 and OR1 samples in all systems. The formulations containing jojoba and grape seed oils were the most susceptible to separation, retaining only 25 to 35% of the emulsified phase at the end of the storage period, while the system with castor oil showed slightly superior performance (FR5 = 60% and OR1 = 30%). This behavior may be associated with the higher viscosity and polarity of castor oil, which favor more effective interactions between the oil phase and the cellulose fibrils.

3.2.4. Microscopic Characterization of Emulsions

Figure 4 shows the average volumetric diameters (D_{32}), measured at the beginning and after 60 days of storage, of the Pickering emulsions stabilized by CNFs and CNCs prepared in phosphate buffer (TF) and containing jojoba, castor, and grape seed vegetable oils.

The CNC-containing emulsions resulted in significantly smaller droplets compared to emulsions stabilized with CNFs, which may be attributed to their greater crystalline characteristics and the smaller size of the nanocrystals. On the other hand, the CNF-containing emulsions showed larger droplets, especially when associated with jojoba oil, whose initial values exceeded 280 µm.

The oil type also influenced the droplet size. The formulations with castor oil showed the lowest D_{32} values, especially in CNC-based systems (close to 30 µm). The use of jojoba oil, on the other hand, led to the formation of larger droplets under virtually all conditions, demonstrating lower interfacial affinity with cellulose particles. The use of grape seed oil resulted in intermediate behavior but with a tendency towards instability during storage in CNF-based systems.

Longer storage times revealed significant variations in stability. The CNC emulsions with jojoba oil showed significant diameter growth, from 51.69 µm to 103.35 µm on day 0 for sample FR5, and from 28 µm to 145 µm after 60 days for sample OR1, indicating instability.

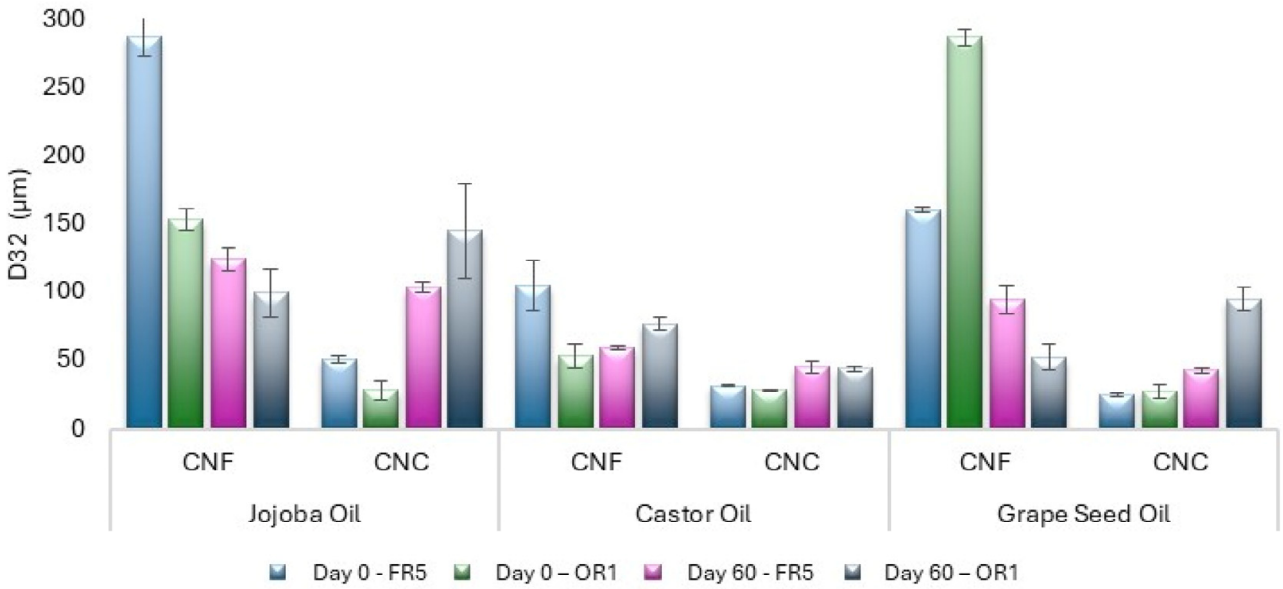

Figure 4. Average volumetric diameters (D_{32}), evaluated on the day of preparation and after 60 days, of Pickering emulsions stabilized by bacterial cellulose nanofibers (CNFs) and bacterial cellulose nanocrystals (CNCs) formulated with jojoba, castor, and grape seed oils under optimal fiber (FR) and oil (OR) ratio conditions. FR5 samples: oil/water emulsion at a 15% (v/v) ratio prepared with 10 mM phosphate buffer containing 0.09% nanofibers. OR1 samples: 0.05% (w/v) nanocrystal emulsion prepared in 10 mM phosphate buffer containing 5% (v/v) oil.

It is notable that sample OR1 produced smaller droplets and more stable emulsions compared to sample FR5. This can be attributed to the greater availability of cellulose particles to coat the interface, which decreases droplet coalescence.

These results support recent studies showing that Pickering emulsions stabilized by cellulose mainly result in microemulsions, with typical diameters ranging from 0.1 to 100 µm [63]. Hossain et al. [64] emphasized that the presence of CNCs favors the formation of smaller, more stable droplets due to their high surface area-to-volume ratio and dense surface charges. This is also demonstrated by the smaller droplet sizes observed in this study for CNC-based emulsions compared to those stabilized by CNFs. Similarly, Guzmán et al. [65] reported that smaller droplets have greater interfacial coverage with solid particles, leading to systems more resistant to coalescence. This explains the higher stability with lower oil ratios seen in this study, especially in the systems made with castor oil. Additionally, Rosdianto et al. [66] pointed out that both the medium composition and the type of oil directly affect emulsion stability, suggesting that systems with higher ionic strength may behave differently.

3.3. Cosmetic Formulations

Three different cosmetic formulations were prepared: two containing CNCs—one with PEG-7 glyceryl cocoate and one without—plus a third formulation without CNCs, which was used as a control. PEG-7 glyceryl cocoate was selected because it is a non-ionic surfactant with emulsifying and emollient properties, and is commonly used in hair and skin care products [67]. All formulations remained physically stable throughout the storage period, showing no visible phase separation from preparation to 7 days of storage (Figure 5). The centrifugation test (3000 rpm for 15 min at room temperature) confirmed these findings as there were no signs of physical instability.

Figure 5. Visual appearance of the emulsified conditioning formulations after 7 days of storage. Bacterial cellulose nanocrystal (CNC) formulations with (A) and without (B) PEG-7 glyceryl cocoate; (C) control formulation without CNCs.

Despite similar stability, clear differences were observed in the visual appearance and consistency of the formulations. The control formulation appeared more fluid, while the one containing CNCs and PEG-7 glyceryl cocoate had an intermediate creamy consistency. Conversely, the CNC-based formulation without PEG-7 glyceryl cocoate showed the thickest consistency, behaving as a dense, structured cream. This suggests that nanocrystal incorporation affected the internal organization of the system (Figure 6).

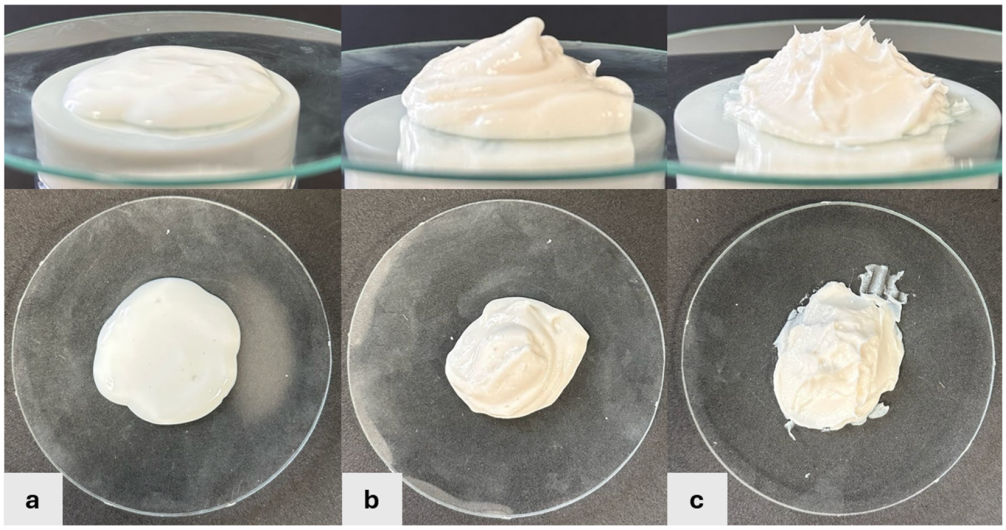

Figure 6. Visual comparison of the different textures of moisturizing cream formulations (top and side views). (**a**) Control formulation without bacterial cellulose nanocrystals (CNCs); (**b**) formulation containing CNCs and PEG-7 glyceryl cocoate; (**c**) formulation containing CNCs without PEG-7 glyceryl cocoate.

The absence of nanocrystals caused the emulsion to be thermally unstable, so raising the temperature to 60 °C sped up the destabilization, leading to phase separation after 12 h (Figure 7). In contrast, the CNC-based formulations remained stable, showing that nanocrystalline BC effectively served as a stabilizing agent, possibly through Pickering-type stabilization by forming a physical barrier around the droplets and increasing the resistance to coalescence under thermal stress.

Figure 7. Visual comparison of the stability of moisturizing cream formulations under the influence of temperature (4 °C on the **left** and 60 °C on the **right**). (**A**) Control formulation without bacterial cellulose nanocrystals (CNCs); (**B**) formulation containing CNCs and PEG-7 glyceryl cocoate; (**C**) formulation containing CNCs without PEG-7 glyceryl cocoate.

The stability seen at 4 °C, even in the emulsion without CNCs, indicates that the low temperature reduced molecular mobility, lowered the collision frequency among droplets, and increased the system's viscosity, thereby delaying destabilization processes. These results, which should not be attributed to the formulation itself but rather to favorable storage conditions, show that the nanocrystals provided additional thermal stability to the emulsion, which is particularly important under stress conditions such as high temperatures.

The formulations' moisture content varied depending on the presence of BC and the system composition. The control formulation and the one containing CNCs and PEG-7 glyceryl cocoate showed 68.92 and 68.07% moisture, respectively, while the CNC-based formulation without PEG-7 glyceryl cocoate maintained a moisture content (71.39%) compatible with the initial composition, indicating that the cellulose nanocrystals were able to retain water in the emulsified matrix even in the absence of an additional hydrophilic emollient.

These results relate to the hydrophilic properties of BC nanocrystals and the pretreatment of the material with additive-assisted drying based on ethanol–water solvent exchange. This process reduced the excess free water content in the BC and adjusted its pH to about 5, promoting its incorporation into the emulsified matrix. Controlled rehydration of the fibers helped retain water in the system without damaging the physical stability of the formulations.

Viscosity analysis showed notable differences among the formulations. The control formulation, which lacked CNCs and contained PEG-7 glyceryl cocoate, displayed the lowest apparent viscosity (4077 mPa·s), indicating its more fluid nature. Adding CNCs led to a significant increase in viscosity, reaching 9434 and 10,562 mPa·s in the formulations with and without PEG-7 glyceryl cocoate, respectively. These values were close to or within the range (10,000–50,000 mPa·s) deemed suitable for cosmetic creams [68], while the control remained below this recommended range.

These results demonstrate the structuring role of nanocrystals in improving product consistency in the emulsified system. The absence of PEG-7 glyceryl cocoate did not affect system stability due to the increased viscosity, emphasizing the functional role of the fibers in structuring the emulsion.

A comparison of CNC-based formulations with and without PEG-7 glyceryl cocoate shows that the absence of this synthetic additive did not affect the physical stability or rheological behavior of the system. The formulation without PEG-7 glyceryl cocoate had a higher apparent viscosity, indicating that cellulose nanocrystals mainly contributed to structuring the emulsion. This effect is due to the properties of cellulose nanocrystals,

such as their nanometer size, high surface area, and ability to interact with the oil–water interface, which promote system stabilization and texture modulation.

The prototype conditioning cosmetic formulation was developed to assess the behavior and suitability of the cellulose-based polymer within a complex cosmetic matrix. This approach aimed to verify whether incorporating cellulose nanocrystals, alongside other formulation components, could promote structural organization and affect the rheological properties of the emulsified system. The observations obtained provide a qualitative indication of the structuring role of cellulose nanocrystals within the emulsion system, which is in line with previous reports [69–71]. At this stage, the evaluation was limited to physicochemical stability and rheological behavior, and no quantitative assessments of sensory attributes or conditioning effectiveness were conducted.

Safety-related aspects were not experimentally addressed; however, bacterial cellulose-based materials have been widely reported in the literature as biocompatible and non-cytotoxic when properly purified and used within appropriate concentration ranges [72–74].

4. Conclusions

The reproducible production of bacterial cellulose under controlled conditions allows for the consistent creation of fibrous materials suitable for subsequent hydrolytic processing. Structural and physicochemical analyses confirmed that the type of hydrolysis used results in significant differences in the performance of bacterial cellulose (BC) fibers as Pickering emulsion stabilizers. Bacterial cellulose nanocrystals (CNCs) produced through sulfuric hydrolysis showed greater crystallinity, uniform dimensions, and a surface modified by sulfate groups. These characteristics enhance their negative charge and electrostatic stability, promoting interfacial adsorption and leading to more stable emulsions, regardless of the oil used, with particularly superior performance using castor oil.

Although bacterial cellulose nanofibers (CNFs) produced by hydrochloric acid hydrolysis exhibited a smaller average size, their lower colloidal uniformity and the presence of free ions reduced their efficiency as stabilizers in long-term systems. Thus, sulfation of BC appears to be an effective strategy to improve the colloidal behavior of the fibers and expand their applicability in cosmetic and food formulations.

Overall, the results of this study demonstrate the potential of CNC-based systems as high-performance natural stabilizers, aiding in the development of more stable Pickering emulsions that support the goals of green cosmetics and replacing synthetic additives.

The presence of CNCs helped structure the emulsion and adjust the formulation's physicochemical properties, enabling the replacement of PEG-7 glyceryl cocoate, a synthetic non-ionic surfactant with emulsifying and emollient functions. The formulation without this ingredient exhibited better performance in stability and structural organization, showing that BC derivatives can perform technological functions usually linked to synthetic additives. These findings highlight the potential of CNCs as a sustainable and functional alternative in developing innovative cosmetics, supporting the principles of clean beauty, reducing synthetic inputs, and emphasizing renewable raw materials.

Supplementary Materials: The following supporting information can be downloaded at: https://www.mdpi.com/article/10.3390/cosmetics13010031/s1, Table S1: Emulsification index (%) of samples prepared in triplicate with different fiber (FR) and oil (OR) ratios. The emulsion tests were performed over 7 days with jojoba oil, using nanofiber obtained by hydrolysis with HCl. Data are presented as mean ± standard deviation. FR samples: oil/water emulsions in a 15% (v/v) ratio, prepared with 10 mM phosphate buffer containing nanofiber concentrations (w/v) of 0.01% (FR1), 0.03% (FR2), 0.05% (FR3), 0.07% (FR4), and 0.09% (FR5). OR samples: 0.05% (w/v) nanofiber emulsions, prepared with 10 mM phosphate buffer containing oil-in-water (v/v) concentrations of 5% (OR1), 10% (OR2), 15% (OR3), 20% (OR4), 25% (OR5), and 30% (OR6);

Table S2: Emulsification index (%) of samples prepared in triplicate with different fiber (FR) and oil (OR) ratios. The emulsion tests were performed over 7 days with castor oil, using nanofiber obtained by hydrolysis with HCl. Data are presented as mean ± standard deviation. FR samples: oil/water emulsions in a 15% (v/v) ratio, prepared with 10 mM phosphate buffer containing nanofiber concentrations (w/v) of 0.01% (FR1), 0.03% (FR2), 0.05% (FR3), 0.07% (FR4), and 0.09% (FR5). OR samples: 0.05% (w/v) nanofiber emulsions, prepared with 10 mM phosphate buffer containing oil-in-water (v/v) concentrations of 5% (OR1), 10% (OR2), 15% (OR3), 20% (OR4), 25% (OR5), and 30% (OR6); Table S3: Emulsification index (%) of samples prepared in triplicate with different fiber (FR) and oil (OR) ratios. The emulsion tests were performed over 7 days with grape seed oil, using nanofiber obtained by hydrolysis with HCl. Data are presented as mean ± standard deviation. FR samples: oil/water emulsions in a 15% (v/v) ratio, prepared with 10 mM phosphate buffer containing nanofiber concentrations (w/v) of 0.01% (FR1), 0.03% (FR2), 0.05% (FR3), 0.07% (FR4), and 0.09% (FR5). OR samples: 0.05% (w/v) nanofiber emulsions, prepared with 10 mM phosphate buffer containing oil-in-water (v/v) concentrations of 5% (OR1), 10% (OR2), 15% (OR3), 20% (OR4), 25% (OR5), and 30% (OR6); Table S4: Emulsification index (%) of samples prepared in triplicate with different fiber (FR) and oil (OR) ratios. The emulsion tests were performed over 7 days with jojoba oil, using nanocrystals obtained by hydrolysis with H_2SO_4. Data are presented as mean ± standard deviation. FR samples: oil/water emulsions in a 15% (v/v) ratio, prepared with 10 mM phosphate buffer containing nanofiber concentrations (w/v) of 0.01% (FR1), 0.03% (FR2), 0.05% (FR3), 0.07% (FR4), and 0.09% (FR5). OR samples: 0.05% (w/v) nanofiber emulsions, prepared with 10 mM phosphate buffer containing oil-in-water (v/v) concentrations of 5% (OR1), 10% (OR2), 15% (OR3), 20% (OR4), 25% (OR5), and 30% (OR6); Table S5: Emulsification index (%) of samples prepared in triplicate with different fiber (FR) and oil (OR) ratios. The emulsion tests were performed over 7 days with castor oil, using nanocrystals obtained by hydrolysis with H_2SO_4. Data are presented as mean ± standard deviation. FR samples: oil/water emulsions in a 15% (v/v) ratio, prepared with 10 mM phosphate buffer containing nanofiber concentrations (w/v) of 0.01% (FR1), 0.03% (FR2), 0.05% (FR3), 0.07% (FR4), and 0.09% (FR5). OR samples: 0.05% (w/v) nanofiber emulsions, prepared with 10 mM phosphate buffer containing oil-in-water (v/v) concentrations of 5% (OR1), 10% (OR2), 15% (OR3), 20% (OR4), 25% (OR5), and 30% (OR6); Table S6: Emulsification index (%) of samples prepared in triplicate with different fiber (FR) and oil (OR) ratios. The emulsion tests were performed over 7 days with grape seed oil, using nanocrystals obtained by hydrolysis with H_2SO_4. Data are presented as mean ± standard deviation. FR samples: oil/water emulsions in a 15% (v/v) ratio, prepared with 10 mM phosphate buffer containing nanofiber concentrations (w/v) of 0.01% (FR1), 0.03% (FR2), 0.05% (FR3), 0.07% (FR4), and 0.09% (FR5). OR samples: 0.05% (w/v) nanofiber emulsions, prepared with 10 mM phosphate buffer containing oil-in-water (v/v) concentrations of 5% (OR1), 10% (OR2), 15% (OR3), 20% (OR4), 25% (OR5), and 30% (OR6); Table S7: Effect of pH on the emulsification index (%) of emulsions prepared in triplicate using the best fiber (FR) and oil (OR) ratios. The emulsion tests were performed over 7 days with jojoba, castor and grape seed oils, using nanofiber obtained by hydrolysis with HCl. Data are presented as mean ± standard deviation. FR5 sample: oil/water emulsion in a 15% (v/v) ratio, prepared with 10 mM phosphate buffer containing nanofiber concentration of 0.09% (w/v). OR1 sample: 0.05% (w/v) nanofiber emulsion, prepared with 10 mM phosphate buffer containing oil-in-water concentration of 5% (v/v); Table S8: Effect of temperature on the emulsification index (%) of emulsions prepared in triplicate using the best fiber (FR) and oil (OR) ratios. The emulsion tests were performed over 7 days with jojoba, castor and grape seed oils, using nanofiber obtained by hydrolysis with HCl. Data are presented as mean ± standard deviation. FR5 sample: oil/water emulsion in a 15% (v/v) ratio, prepared with 10 mM phosphate buffer containing nanofiber concentration of 0.09% (w/v). OR1 sample: 0.05% (w/v) nanofiber emulsion, prepared with 10 mM phosphate buffer containing oil-in-water concentration of 5% (v/v); Table S9: Effect of pH on the emulsification index (%) of emulsions prepared in triplicate using the best fiber (FR) and oil (OR) ratios. The emulsion tests were performed over 7 days with jojoba, castor and grape seed oils, using nanocrystals obtained by hydrolysis with H_2SO_4. Data are presented as mean ± standard deviation. FR5 sample: oil/water emulsion in a 15% (v/v) ratio, prepared with

10 mM phosphate buffer containing nanofiber concentration of 0.09% (*w*/*v*). OR1 sample: 0.05% (*w*/*v*) nanofiber emulsion, prepared with 10 mM phosphate buffer containing oil-in-water concentration of 5% (*v*/*v*); Table S10: Effect of temperature on the emulsification index (%) of emulsions prepared in triplicate using the best fiber (FR) and oil (OR) ratios. The emulsion tests were performed over 7 days with jojoba, castor and grape seed oils, using nanocrystals obtained by hydrolysis with H_2SO_4. Data are presented as mean ± standard deviation. FR5 sample: oil/water emulsion in a 15% (*v*/*v*) ratio, prepared with 10 mM phosphate buffer containing nanofiber concentration of 0.09% (*w*/*v*). OR1 sample: 0.05% (*w*/*v*) nanofiber emulsion prepared with 10 mM phosphate buffer containing oil-in-water concentration of 5% (*v*/*v*).

Author Contributions: Conceptualization, L.A.S. and I.J.B.D.; methodology, A.J.V.d.M.S., D.T.d.S., M.R.d.S., G.P.d.A., and I.J.B.D.; investigation, A.J.V.d.M.S., D.T.d.S., M.R.d.S., G.P.d.A., and A.F.d.S.C.; writing—original draft preparation, A.J.V.d.M.S., D.T.d.S., M.R.d.S., and G.P.d.A.; writing—review and editing, I.J.B.D., A.C., A.F.d.S.C., and L.A.S.; visualization, I.J.B.D., A.C., and L.A.S.; supervision, L.A.S., I.J.B.D., and A.F.d.S.C.; project administration, L.A.S.; funding acquisition, L.A.S. All authors have read and agreed to the published version of the manuscript.

Funding: This study was funded by the Brazilian fostering agencies Fundação de Apoio à Ciência e Tecnologia do Estado de Pernambuco (FACEPE [State of Pernambuco Support to Science and Technology Foundation]), Conselho Nacional de Desenvolvimento Científico e Tecnológico (CNPq [National Council of Scientific and Technological Development]), and Coordenação de Aperfeiçoamento de Pessoal de Nível Superior (CAPES [Coordination for the Advancement of Higher Education Staff]) (Finance Code 001).

Institutional Review Board Statement: Not applicable.

Data Availability Statement: The original contributions presented in the study are included in the article; further inquiries can be directed to the corresponding author.

Acknowledgments: The authors thank the Department of Chemical Engineering of the Federal University of Pernambuco (UFPE), the School of Technology and Communication of the Catholic University of Pernambuco (UNICAP), the Northeast Biotechnology Network (RENORBIO) of the Federal Rural University of Pernambuco (UFRPE), the Department of Textile Engineering of the Federal University of Pernambuco (UFPE), and the Advanced Institute of Technology and Innovation (IATI), Brazil.

Conflicts of Interest: The authors declare no conflicts of interest.

References

1. CNN Brasil. Setor de Cosmético Aposta em Novo Posicionamento para Mercado, Diz Abihpec. Available online: https://www.cnnbrasil.com.br/economia/macroeconomia/setor-de-cosmeticos-apoia-muito-a-reforma-tributaria-diz-abihpec/ (accessed on 1 December 2025).
2. Condezo-Hoyos, L.; Lama-Quispe, S.; Apaza-Medrano, Z.; Cortes-Avendaño, P. Quantification of oil/water emulsion stability kinetics using image analysis: ImageScan method. *Food Chem.* **2025**, *499*, 147094. [CrossRef]
3. Fan, C.; Li, J.; Qu, Z.; Tang, Z.; Zhang, J.; Jiang, H.; Xing, W.; Chen, R. Continuous preparation of stable oil-in-water emulsions by secondary membrane emulsification without surfactants. *Chin. J. Chem. Eng.* **2025**, *87*, 288–298. [CrossRef]
4. Alavi, F.; Ciftci, O.N. Protein aerogels as dual-function carriers: Curcumin delivery and fish oil oleogelation for structured emulsions. *Food Hydrocoll.* **2025**, *173*, 112044. [CrossRef]
5. Dickinson, E. Strategies to control and inhibit the flocculation of protein-stabilized oil-in-water emulsions. *Food Hydrocoll.* **2019**, *96*, 209–223. [CrossRef]
6. Zou, Y.; Hu, H.; Huang, Z.; Dong, H.; Peng, S.; Li, R.; Fu, T.; Rao, J.; Zheng, L.; Huang, X.; et al. Pickering emulsions stabilized by moringa seed residue protein/tannic acid particles for curcumin loading: Enhanced retention and bioaccessibility. *Food Chem. X* **2025**, *32*, 103304. [CrossRef] [PubMed]
7. McWilliams, J.B.; Kinoshita, H.; Walkley, B.; Provis, J.L. Immobilising oils in geopolymer cements using Pickering emulsions. *Nucl. Eng. Des.* **2025**, *445*, 114530. [CrossRef]
8. Wu, F.; Deng, J.; Hu, L.; Zhang, Z.; Jiang, H.; Li, Y.; Yi, Z.; Ngai, T. Investigation of the stability in Pickering emulsions preparation with commercial cosmetic ingredients. *Colloids Surf. A Physicochem. Eng. Asp.* **2020**, *602*, 125082. [CrossRef]

9. Peito, S.; Peixoto, D.; Ferreira-Faria, I.; Martins, A.M.; Ribeiro, H.M.; Veiga, F.; Marto, J.; Paiva-Santos, A.C. Nano- and microparticle-stabilized Pickering emulsions designed for topical therapeutics and cosmetic applications. *Int. J. Pharm.* **2022**, *615*, 121455. [CrossRef]
10. Tyowua, A.T.; Yiase, S.G.; Binks, B.P. Double oil-in-oil-in-oil emulsions stabilised solely by particles. *J. Colloid Interface Sci.* **2017**, *488*, 127–134. [CrossRef]
11. Teo, S.H.; Chee, C.Y.; Fahmi, M.Z.; Sakti, S.C.W.; Lee, H.V. Review of Functional Aspects of Nanocellulose-Based Pickering Meu sifier for Non-Toxic Application and Its Colloid Stabilization Mechanism. *Molecules* **2022**, *27*, 7170. [CrossRef]
12. Tu, H.; Yu, Y.; Chen, J.J.; Shi, X.W.; Zhou, J.L.; Deng, H.B.; Du, Y.M. Highly cost-effective and high-strength hydrogels as dye adsorbents from natural polymers: Chitosan and cellulose. *Polym. Chem.* **2017**, *8*, 2913–2921. [CrossRef]
13. Rayees, R.; Gani, A.; Noor, N.; Ayoub, A.; Ashraf, Z.U. General approaches to biopolymer-based Pickering emulsions. *Int. J. Biol. Macromol.* **2024**, *267*, 131430. [CrossRef] [PubMed]
14. Morais, J.P.S.; Rosa, M.F.; Brito, E.S.; Azeredo, H.M.C.; Figueirêdo, M.C.B. Sustainable Pickering Emulsions with Nanocellulose: Innovations and Challenges. *Foods* **2023**, *12*, 3599. [CrossRef] [PubMed]
15. Almeida, N.T.; Pereira, A.L.S.; Barros, N.O.; Mattos, A.L.A.; Rosa, M.F. Enhancing Starch Film Properties Using Bacterial Nanocellulose-Stabilized Pickering Emulsions. *Polymers* **2024**, *16*, 3346. [CrossRef] [PubMed]
16. Amorim, J.D.P.; Souza, K.C.; Duarte, C.R.; Duarte, I.S.; Ribeiro, F.A.S.; Silva, G.S.; Farias, P.M.A.; Stingl, A.; Costa, A.F.S.; Vinhas, G.M.; et al. Plant and bacterial nanocellulose: Production, properties and applications in medicine, food, cosmetics, electronics and engineering. A review. *Environ. Chem. Lett.* **2020**, *18*, 851–869. [CrossRef]
17. Amorim, J.D.P.; Silva Junior, C.J.G.; Medeiros, A.D.M.; Nascimento, H.A.; Sarubbo, M.; Medeiros, T.P.M.; Costa, A.F.S.; Sarubbo, L.A. Bacterial cellulose as a versatile biomaterial for wound dressing application. *Molecules* **2022**, *27*, 5580. [CrossRef]
18. Silva Junior, C.J.G.; Medeiros, A.D.M.; Amorim, J.D.P.; Nascimento, H.A.; Converti, A.; Costa, A.F.S.; Sarubbo, L.A. Bacterial cellulose biotextiles for the future of sustainable fashion: A review. *Environ. Chem. Lett.* **2021**, *19*, 2967–2980. [CrossRef]
19. Medeiros, A.D.M.; Silva Junior, C.J.G.; Amorim, J.D.P.; Nascimento, H.A.; Converti, A.; Costa, A.F.S.; Sarubbo, L.A. Bacterial cellulose for treatment of wastewaters generated by energy consuming industries: A review. *Energies* **2021**, *14*, 5066. [CrossRef]
20. Medeiros, A.D.M.; Silva Junior, C.J.G.; Amorim, J.D.P.; Durval, I.J.B.; Costa, A.F.S.; Sarubbo, L.A. Oily wastewater treatment: Methods, challenges, and trends. *Processes* **2022**, *10*, 743. [CrossRef]
21. Don, T.M.; Lee, K.T.; Chen, B.Y.; Tang, S.; Huang, Y.C.; Chuang, A.E.Y. Physicochemical properties of bacterial cellulose/phototherapeutic polypyrrole/antibacterial chitosan composite membranes and their evaluation as chronic wound dressings. *Int. J. Biol. Macromol.* **2025**, *308*, 142186. [CrossRef]
22. Hou, C.L.; Wei, H.T.; Liu, C.; Yang, H.M.; Chen, L.C.; Xu, J.P.; Wang, L.Y.; Rao, X.H.; Huang, J.J.; Ge, Q. Application potential of submicron-sized bamboo cellulose as natural Pickering emulsion stabilizers: Structural properties and stabilization mechanisms. *Food Chem.* **2025**, *489*, 144946. [CrossRef]
23. Souza, T.C.; Amorim, J.D.P.; Silva Junior, C.J.G.; Medeiros, A.D.M.; Costa, A.F.S.; Vinhas, G.M.; Sarubbo, L.A. Magnetic bacterial cellulose biopolymers: Production and potential applications in the electronics sector. *Polymers* **2023**, *15*, 853. [CrossRef]
24. Ebrahimi, R.; Fathi, M.; Ghoddusi, H.B. Pickering emulsions stabilized by cellulose nanocrystals extracted from hazelnut shells: Production and stability under different harsh conditions. *Int. J. Biol. Macromol.* **2024**, *258*, 128982. [CrossRef]
25. Mitbumrung, W.; Matsukawa, S. Cellulose nanocrystal stabilized pickering nanoemulsions and their coalescence stability studied by fluorescence microscopy. *Food Hydrocoll.* **2024**, *149*, 109594. [CrossRef]
26. Yang, J.; Kwon, H.; Jeong, D.; Kim, J.W. Advanced nanocellulose interface engineering for Pickering emulsion stabilization. *Adv. Ind. Eng. Chem.* **2025**, *1*, 25. [CrossRef]
27. Ji, C.; Wang, Y. Nanocellulose-stabilized Pickering emulsions: Fabrication, stabilization, and food applications. *Adv. Colloid Interface Sci.* **2023**, *318*, 102970. [CrossRef]
28. Pinto, N.O.F.; Bourbon, A.I.; Martins, D.; Pereira, A.; Cerqueira, M.A.; Pastrana, L.; Gama, M.; Azeredo, H.M.C.; Rosa, M.F.; Gonçalves, C. Bacterial cellulose nanocrystals or nanofibrils as Pickering stabilizers in low-oil emulsions: A comparative study. *Food Hydrocoll.* **2024**, *157*, 110427. [CrossRef]
29. Medeiros, A.D.M.; Silva Junior, C.J.G.; Cavalcanti, Y.F.; Cavalcanti, M.H.C.; Santos, M.R.; Resende, A.H.M.; Silva, I.A.; Amorim, J.D.P.; Costa, A.F.S.; Sarubbo, L.A. Multifunctional performance of bacterial cellulose membranes in saline and oily emulsion filtration. *Fermentation* **2025**, *11*, 635. [CrossRef]
30. Hestrin, S.; Schramm, M. Synthesis of cellulose by *Acetobacter xylinum*. 2. Preparation of freeze-dried cells capable of polymerizing glucose to cellulose. *Biochem. J.* **1954**, *58*, 345–352. [CrossRef]
31. Costa, A.F.S.; Almeida, F.C.G.; Vinhas, G.M.; Sarubbo, L.A. Production of bacterial cellulose by *Gluconacetobacter hansenii* using corn steep liquor as nutrient sources. *Front. Microbiol.* **2017**, *8*, 2027. [CrossRef]
32. Kalashnikova, I.; Bizot, H.; Cathala, B.; Capron, I. Modulation of cellulose nanocrystals amphiphilic properties to stabilize oil/water interface. *Biomacromolecules* **2012**, *13*, 267–275. [CrossRef]

33. Silva Junior, C.J.G.; Medeiros, A.D.M.; Cavalcanti, A.K.L.d.H.; Amorim, J.D.P.; Durval, I.J.B.; Cavalcanti, Y.F.; Converti, A.; Costa, A.F.S.; Sarubbo, L.A. Towards sustainable packaging using microbial cellulose and sugarcane (*Saccharum officinarum* L.) bagasse. *Materials* **2024**, *17*, 3732. [CrossRef]
34. Cooper, D.G.; Goldenberg, B.G. Surface-active agents from two *Bacillus* species. *Appl. Environ. Microbiol.* **1987**, *53*, 224–229. [CrossRef] [PubMed]
35. Dey, S.; Khan, M.A.; Prakash, S.; Jangid, L.; Joshi, D.; Mandal, A. Synthesis and physicochemical evaluation of an olive oil-derived anionic surfactant: Effects on interfacial tension, wettability alteration, and oil recovery efficiency. *Ind. Eng. Chem. Res.* **2025**, *64*, 16375–16392. [CrossRef]
36. Bezerra, K.G.O.; Meira, H.M.; Veras, B.O.; Stamford, T.C.M.; Fernandes, E.L.; Converti, A.; Rufino, R.D.; Sarubbo, L.A. Application of plant surfactants as cleaning agents in shampoo formulations. *Processes* **2023**, *11*, 879. [CrossRef]
37. Wu, Y.; Lei, C.; Li, J.; Chen, Y.; Liang, H.; Li, Y.; Li, B.; Luo, X.; Pei, Y.; Liu, S. Improvement of O/W emulsion performance by adjusting the interaction between gelatin and bacterial cellulose nanofibrils. *Carbohydr. Polym.* **2022**, *276*, 118806. [CrossRef] [PubMed]
38. Wei, Z.; Liu, L.; Yang, J.; Dunn, C.B.; Zhang, T.; Hong, F.F.; Qiang, Z.; Ren, J. Ethanol-mediated freeze-drying enables robust bacterial cellulose aerogels for enhanced drug loading and hemostasis dressing. *Carbohydr. Polym.* **2025**, *368*, 124091. [CrossRef]
39. Galdino, C.J.S., Jr.; Maia, A.D.; Meira, H.M.; Souza, T.C.; Amorim, J.D.P.; Almeida, F.C.G.; Costa, A.F.S.; Sarubbo, L.A. Use of a bacterial cellulose filter for the removal of oil from wastewater. *Process Biochem.* **2020**, *91*, 288–296. [CrossRef]
40. Bangar, S.P.; Harussani, M.M.; Ilyas, R.A.; Ashogbon, A.O.; Singh, A.; Trif, M.; Jafari, S.M. Surface modifications of cellulose nanocrystals: Processes, properties, and applications. *Food Hydrocoll.* **2022**, *130*, 107689. [CrossRef]
41. Wang, H.; Xie, H.; Du, H.; Wang, X.; Liu, W.; Duan, Y.; Zhang, X.; Sun, L.; Zhang, X.; Si, C. Highly efficient preparation of functional and thermostable cellulose nanocrystals via H_2SO_4 intensified acetic acid hydrolysis. *Carbohydr. Polym.* **2020**, *239*, 116233. [CrossRef]
42. Pang, W.; Han, H.; Zheng, K.; Jiang, L.; Wang, J.; Qian, S. Cellulose nanocrystal-stabilized Pickering emulsion gels as vehicles for follicular delivery of minoxidil. *Int. J. Biol. Macromol.* **2024**, *277*, 134297. [CrossRef]
43. Filippov, S.K.; Khusnutdinov, R.; Murmiliuk, A.; Inam, W.; Zakharova, L.Y.; Zhang, H.; Khutoryanskiy, V.V. Dynamic light scattering and transmission electron microscopy in drug delivery: A roadmap for correct characterization of nanoparticles and interpretation of results. *Mater. Horiz.* **2023**, *10*, 5354. [CrossRef]
44. Chikina, I.; Nakamae, S.; Varlamov, A. On the ac measurements of the electrical conductivity of dilute colloidal electrolytes. *Colloids Interfaces* **2023**, *7*, 58. [CrossRef]
45. Alade, O.S.; Mahmoud, M.; Al-Nakhli, A. Rapid determination of emulsion stability using turbidity measurement incorporating artificial neural network (ANN): Experimental validation using video/optical microscopy and kinetic modeling. *ACS Omega* **2021**, *6*, 5910−5920. [CrossRef] [PubMed]
46. Ferreira, G.S.; Silva, D.J.; Oliveira, E.R.; Rosa, D.S. Oil-in-water Pickering emulsions with *Buriti* vegetable oil stabilized with cellulose nanofibrils: Preparation, stability and antimicrobial Properties. *Int. J. Biol. Macromol.* **2025**, *304*, 140233. [CrossRef]
47. Perrin, L.; Desobry, S.; Gille, G.; Desobry-Banon, S. Low-frequency ultrasound effects on cellulose nanocrystals for potential application in stabilizing Pickering emulsions. *Polymers* **2023**, *15*, 4371. [CrossRef]
48. Aw, Y.Z.; Lim, H.P.; Low, L.E.; Singh, C.K.S.; Chan, E.S.; Tey, B.T. Cellulose nanocrystal (CNC)-stabilized Pickering emulsion for improved curcumin storage stability. *LWT* **2022**, *159*, 113249. [CrossRef]
49. Yuan, T.; Zeng, J.; Wang, B.; Cheng, Z.; Chen, K. Pickering emulsion stabilized by cellulosic fibers: Morphological properties–interfacial stabilization–rheological behavior relationships. *Carbohydr. Polym.* **2021**, *269*, 118339. [CrossRef]
50. Meng, W.; Sun, H.; Mu, T.; Garcia-Vaquero, M. Future trends in the field of Pickering emulsions: Stabilizers, spray-dried microencapsulation and rehydration for food applications. *Trends Food Sci. Technol.* **2024**, *150*, 104610. [CrossRef]
51. Guan, X.; Jiang, H.; Lin, J.; Ngai, T. Pickering emulsions: Microgels as alternative surfactants. *Curr. Opin. Colloid Interface Sci.* **2024**, *73*, 101827. [CrossRef]
52. Song, Y.; Im, S.H. Highly crystalline poly-3-hexylthiophene particles prepared from Pickering emulsions stabilized by alkylamine functionalized graphene quantum dots. *Colloids Surf. A Physicochem. Eng. Asp.* **2024**, *701*, 134819. [CrossRef]
53. Ybanez, M.G.; Camacho, D.H. Designing hydrophobic bacterial cellulose film composites assisted by sound waves. *RSC Adv.* **2021**, *11*, 32873–32883. [CrossRef]
54. Carvalho-Guimarães, F.B.; Correa, K.L.; Souza, T.P.; Amado, J.R.R.; Ribeiro-Costa, R.M.; Silva-Junior, J.O. A review of Pickering emulsions: Perspectives and applications. *Pharmaceuticals* **2022**, *15*, 1413. [CrossRef]
55. Tan, Y.; Wu, P.; Yu, J.; Bai, J.; Nie, C.; Liu, B.; Niu, Y.; Fan, G.; Wang, J. Stabilization of Pickering emulsions with bacterial cellulose nanofibrils (BCNFs) fabricated by electron beam irradiation. *Innov. Food Sci. Emerg. Technol.* **2024**, *94*, 103664. [CrossRef]
56. Rajak, A.K.; Harikrishna, M.; Sarangi, P.K.; Prus, P.; Karuna, M.S.L. Biolubricant production from Indian castor seed oil using ethyl biodiesel (2G precursor) and sodium methoxide as a homogeneous catalyst. *Mol. Catal.* **2026**, *591*, 115–697. [CrossRef]

57. Vu, G.M.; Tran, N.H.; Tran, M.P.L.; Dam, A.N.; Lieu, N.N.; Nguyen, N.M.; Ngo, N.Y.L.; Dinh, T.N.N.; Nguyen, D.Q. Saponin-stabilized nanoemulsions co-encapsulating grape seed oil and rosemary essential oil: Formulation, characterization, stability, and antioxidant capacity. *J. Mol. Liq.* **2025**, *437*, 128495. [CrossRef]
58. Sarkar, K.; Pandit, Y.B.; Massarwa, A.; Lemcoff, N.G.; Reany, O. Precipitation driven ADMET polymerization of jojoba oil for recyclable biorenewable polymers. *Eur. Polym. J.* **2025**, *239*, 114297. [CrossRef]
59. Chen, A.; Zhou, S.; Kong, Y.; Han, W.; Li, X.; Cai, X. Enhanced emulsification of cellulose nanocrystals by ε-polylysine to stabilize Pickering emulsions. *Int. J. Biol. Macromol.* **2024**, *260*, 128940. [CrossRef] [PubMed]
60. Son, H.K.; Park, S.C.; Kim, J.-C. Emulsions stabilized with an electrostatic complex of quaternized cellulose nanofiber and octanoyl gelatin and the effect of pH value on their stability. *Appl. Sci.* **2024**, *14*, 4122. [CrossRef]
61. Abedi, S.; Chen, C.C.; Vanapalli, S.A. Catastrophic thermal destabilization of two-dimensional close-packed emulsions due to synchronous coalescence initiation. *Soft Matter* **2020**, *16*, 6032–6037. [CrossRef]
62. Zhang, W.; Li, J.; Wang, Y.; Ou, W.; Zhu, G.; Zheng, S. Pickering emulsions stabilized by modified Thanaka powder: Emulsifying capability and stability. *Green Sci.* **2025**, *27*, 44–53. [CrossRef]
63. Franceschini, M.; Pizzetti, F.; Rossi, F. On the key role of polymeric rheology modifiers in emulsion-based cosmetics. *Cosmetics* **2025**, *12*, 76. [CrossRef]
64. Hossain, K.M.Z.; Deeming, L.; Edler, K.J. Recent progress in Pickering emulsions stabilised by bioderived particles. *RSC Adv.* **2021**, *11*, 39027–39044. [CrossRef]
65. Guzmán, E.; Ortega, F.; Rubio, R.G. Pickering Emulsions: A Novel Tool for Cosmetic Formulators. *Cosmetics* **2022**, *9*, 68. [CrossRef]
66. Rosdianto, R.S.; Zakiyah, N.; Viviani, R.N.; Deisberanda, F.S.; Nareswari, T.L.; Satrialdi, I.; Fidrianny, I.; Adhika, D.R.; Waresindo, W.X.; Supratman, U.; et al. Novel insight into pickering emulsion and colloidal particle network construction of basil extract for enhancing antioxidant and UV-B-induced antiaging activities. *ACS Omega* **2023**, *8*, 15932–15950. [CrossRef] [PubMed]
67. Najih, Y.A.; Rakhma, D.N.; Nailufa, Y.; Prasetyowat, R.D. The effect of vegetable oil combination and surfactant PEG 7 glyceryl cocoate ratio on physical characteristics and physical stability of arbutin microemulsion. *Rom. J. Pharm. Pract.* **2020**, *13*, 52. [CrossRef]
68. SPLABOR. Controle de Viscosidade em Cosmético: Métodos e Importância. Available online: https://www.splabor.com.br/blog/guia-do-comprador/controle-de-viscosidade-em-cosmeticos-metodos-e-importancia/ (accessed on 18 December 2025).
69. Macêdo, A.L.S.; Oliveira, C.J.; Ribeiro, D.T.; Sousa, V.F.; Coêlho, M.L. Quality of the chemical substance of hair straighteners. *Res. Soc. Dev.* **2021**, *10*, e17101421424. [CrossRef]
70. Silva, D.A.; Carmo, E.S.; Azevedo, M.G.B.; Souza, J.B.P. Evaluation of antidandruff shampoo quality. *Infarma* **2018**, *30*, 158–167. [CrossRef]
71. Badi, K.A.; Khan, S.A. Formulation, evaluation and comparison of the herbal shampoo with the commercial shampoos. *Beni-Suef Univ. J. Basic Appl. Sci.* **2014**, *3*, 301–305. [CrossRef]
72. Utoiu, E.; Manoiu, V.S.; Oprita, E.L.; Craciunescu, O. Bacterial cellulose: A sustainable source for hydrogels and 3D-printed scaffolds for tissue engineering. *Gels* **2024**, *10*, 387. [CrossRef]
73. Ciftci, F. Bioadhesion, antimicrobial activity, and biocompatibility evaluation bacterial cellulose based silver nanoparticle bioactive composite films. *Process Biochem.* **2024**, *137*, 99–110. [CrossRef]
74. Oliveira, T.J.; Segato, T.C.M.; Chacon, A.C.; Caetano, E.L.A.; Baldo, D.A.; Grotto, D.; Jozala, A.F. Bacterial cellulose as a sustainable vehicle for the controlled release of nisin and mandelic acid: A clean beauty-based approach for acne treatment. *J. Dermatol. Sci. Cosmet. Technol.* **2025**, *2*, 100121. [CrossRef]